RESEARCH ARTICLE

α_1-Adrenergic receptor–PKC–Pyk2–Src signaling boosts L-type Ca^{2+} channel $Ca_V1.2$ activity and long-term potentiation in rodents

Kwun Nok Mimi Man[1], Peter Bartels[1†], Peter B Henderson[1†], Karam Kim[1], Mei Shi[2], Mingxu Zhang[1,2], Sheng-Yang Ho[1], Madeline Nieves-Cintron[1], Manuel F Navedo[1], Mary C Horne[1,2]*, Johannes W Hell[1,2]*

[1]Department of Pharmacology, University of California, Davis, United States; [2]Department of Pharmacology, University of Iowa, Iowa City, United States

Abstract The cellular mechanisms mediating norepinephrine (NE) functions in brain to result in behaviors are unknown. We identified the L-type Ca^{2+} channel (LTCC) $Ca_V1.2$ as a principal target for G_q-coupled α_1-adrenergic receptors (ARs). α_1AR signaling increased LTCC activity in hippocampal neurons. This regulation required protein kinase C (PKC)-mediated activation of the tyrosine kinases Pyk2 and, downstream, Src. Pyk2 and Src were associated with $Ca_V1.2$. In model neuroendocrine PC12 cells, stimulation of PKC induced tyrosine phosphorylation of $Ca_V1.2$, a modification abrogated by inhibition of Pyk2 and Src. Upregulation of LTCC activity by α_1AR and formation of a signaling complex with PKC, Pyk2, and Src suggests that $Ca_V1.2$ is a central conduit for signaling by NE. Indeed, a form of hippocampal long-term potentiation (LTP) in young mice requires both the LTCC and α_1AR stimulation. Inhibition of Pyk2 and Src blocked this LTP, indicating that enhancement of $Ca_V1.2$ activity via α_1AR–Pyk2–Src signaling regulates synaptic strength.

***For correspondence:** mhorne@ucdavis.edu (MCH); jwhell@ucdavis.edu (JWH)

[†]These authors contributed equally to this work

Competing interest: The authors declare that no competing interests exist.

Funding: See page 26

Received: 21 April 2022
Preprinted: 03 July 2022
Accepted: 19 June 2023
Published: 20 June 2023

Reviewing Editor: Yukiko Goda, Okinawa Institute of Science and Technology, Japan

Editor's evaluation

This study reports of a new signaling pathway in hippocampal neurons by which α_1 receptors for norepinephrine regulate Cav1.2 calcium channels; activation of α_1 receptors enhances a form of long-lasting synaptic plasticity that is dependent on L-type calcium channels. The experiments are comprehensive and well-executed, and the main conclusions are compellingly supported by the data shown. The work has significance for the field of neuroscience in general and for cellular mechanisms of neuroregulation in particular.

Introduction

Norepinephrine (NE) causes arousal and augments behavioral acuity and learning (***Berman and Dudai, 2001***; ***Cahill et al., 1994***; ***Carter et al., 2010***; ***Hu et al., 2007***; ***Minzenberg et al., 2008***). NE signals via the G_q-coupled α_1-adrenergic receptor (AR), G_i-coupled α_2AR, and G_s-coupled β_1, β_2, and β_3 ARs. βARs act through adenylyl cyclase (AC), cAMP, and PKA (***Sanderson and Dell'Acqua, 2011***). The β_2AR, G_s, AC, and PKA are all associated with the L-type Ca^{2+} channel (LTCC) $Ca_V1.2$ for efficient signaling in neurons (***Davare et al., 2001***; ***Dittmer et al., 2014***; ***Murphy et al., 2014***; ***Oliveria et al., 2007***; ***Patriarchi et al., 2016***; ***Qian et al., 2017***) and heart (***Balijepalli et al., 2006***). The formation of this signaling complex identifies $Ca_V1.2$ as a major effector of signaling by NE. We now find that $Ca_V1.2$ is also a major effector for signaling via the α_1AR, which has a higher affinity for NE than

βARs (**Giustino and Maren, 2018**; **Ramos and Arnsten, 2007**). Importantly, a large body of evidence implicates the α_1AR in NE's role in attention and vigilance (**Bari and Robbins, 2013**; **Berridge et al., 2012**; **Hahn and Stolerman, 2005**; **Hvoslef-Eide et al., 2015**; **Liu et al., 2009**; **Puumala et al., 1997**; **Robbins, 2002**).

$Ca_V1.2$ fulfills a remarkably broad spectrum of functions. Dysfunctions due to mutations in $Ca_V1.2$ span from impaired cardiac contractility to the autistic-like behaviors seen in Timothy syndrome (**Splawski et al., 2004**). Furthermore, $Ca_V1.2$ has been linked to filopodia formation in invasive cancer cells (**Jacquemet et al., 2016**). $Ca_V1.2$ is by far the most abundant LTCC in heart and accounts for ~80% of all LTCCs in brain (**Hell et al., 1993a**; **Sinnegger-Brauns et al., 2004**). It governs the heartbeat, vascular tone, and neuronal functions including long-term potentiation (LTP) (**Ghosh et al., 2017**; **Grover and Teyler, 1990**; **Moosmang et al., 2005**; **Patriarchi et al., 2016**; **Qian et al., 2017**), long-term depression (**Bolshakov and Siegelbaum, 1994**), neuronal excitability (**Berkefeld et al., 2006**; **Marrion and Tavalin, 1998**), and gene expression (**Dolmetsch et al., 2001**; **Li et al., 2016**; **Li et al., 2012**; **Ma et al., 2014**; **Marshall et al., 2011**; **Murphy et al., 2014**; **Wheeler et al., 2012**). Studies on $Ca_V1.2$ mutant mice suggest that this channel plays a central role in anxiety disorders, depression, and self-injurious behavior (**Sinnegger-Brauns et al., 2004**). Congruently, LTCC blockers elicit antidepressant effects while agonists induce depression-like behavior (**Mogilnicka et al., 1987**; **Mogilnicka et al., 1988**) and self-biting in mice, a symptom associated with autism (**Jinnah et al., 1999**).

$Ca_V1.2$ consists of the pore-forming subunit $\alpha_1$1.2, a β subunit and the $\alpha_2\delta$ subunit (**Catterall, 2000**; **Dai et al., 2009**; **Zamponi et al., 2015**). The β and $\alpha_2\delta$ subunits facilitate release of $\alpha_1$1.2 subunits from the endoplasmic reticulum, inhibit ubiquitin-mediated degradation of voltage-gated calcium channels, influence electrophysiological properties of Ca^{2+} channels, such as activation and inactivation, and play diverse roles in the regulation of these channels (**Catterall, 2000**; **Dai et al., 2009**; **Zamponi et al., 2015**).

In the cardiovascular system, the α_1AR, the endothelin receptor ET1, and the angiotensin receptor AT_1 are important regulators of LTCC currents via G_q signaling (**Catterall, 2000**; **Kamp and Hell, 2000**; **Voelker et al., 2023**). G_q stimulates phospholipase C-β to induce production of diacylglycerol (DAG) and inositol-1,4,5-trisphosphate (IP_3), which triggers Ca^{2+} release from intracellular stores. DAG and Ca^{2+} act in concert with phosphatidyl-serine to activate different PKC isoforms. Stimulation of PKC mostly leads to an increase in $Ca_V1.2$ activity (**Bkaily et al., 1995**; **Dai et al., 2009**; **Döşemeci et al., 1988**; **He et al., 2000**; **Kamp and Hell, 2000**; **Lacerda et al., 1988**; **Navedo et al., 2005**). However, an inhibitory effect of PKC on $Ca_V1.2$ currents has been reported in cardiomyocytes (**Cheng et al., 1995**; **Voelker et al., 2023**). This inhibition is mediated by phosphorylation of residues T27 and T31 by PKC in an isoform of $\alpha_1$1.2 that is expressed in heart (**McHugh et al., 2000**). T27/T31 are not present in the most prevalent brain isoform due to alternative splicing (**Snutch et al., 1991**); thus, the inhibitory effect of PKC on LTCC currents is typically absent in neurons and neural crest-derived PC12 cells, or in vascular smooth muscle (**Navedo et al., 2005**; **Taylor et al., 2000**). Here, we show that stimulation of the α_1AR and of PKC consistently augments LTCC in hippocampal neurons.

Despite the prominent role of PKC in augmentation of $Ca_V1.2$ activity, how PKC mediates this effect has been unknown. PKC activates the nonreceptor tyrosine kinase Pyk2, a signaling process first shown in PC12 cells (**Dikic et al., 1996**; **Lev et al., 1995**) and later primary neurons (**Bartos et al., 2010**; **Huang et al., 2001**), and cardiomyocytes (**Sabri et al., 1998**). Activation of PKC triggers autophosphorylation of residue Y402 on Pyk2 to create a binding site for the SH2 domain of Src, which upon binding to Pyk2 becomes activated (**Dikic et al., 1996**). Src increases LTCC activity in smooth muscle cells (**Gui et al., 2006**; **Hu et al., 1998**; **Wu et al., 2001**), retinal pigment epithelium (**Strauss et al., 1997**), and neurons (**Bence-Hanulec et al., 2000**; **Endoh, 2005**; **Gui et al., 2006**). Furthermore, PKC (**Navedo et al., 2008**; **Yang et al., 2005**) and Src (**Bence-Hanulec et al., 2000**; **Chao et al., 2011**; **Hu et al., 1998**) are physically and functionally associated with $Ca_V1.2$. These findings underscore the physiological relevance of Src in regulating $Ca_V1.2$. Importantly, the pathway by which Src is activated in the context of $Ca_V1.2$ regulation has not been determined.

Once we established that stimulation of PKC or the G_q/PKC-coupled α_1AR strongly augments LTCC activity in neurons, we tested whether Pyk2 mediates this upregulation of channel activity. We link the α_1AR–PKC signaling to Src, which thus emerges as an important mediator of tyrosine phosphorylation on $Ca_V1.2$ downstream of G_q-coupled receptors. In neurons, the nearly twofold increase in LTCC currents upon stimulation of PKC with phorbol-12-myristate-13-acetate (PMA) or via the α_1AR was

blocked by inhibitors of Pyk2 and Src, consistent with earlier data showing that Src elevates $Ca_V1.2$ activity to a comparable degree (***Bence-Hanulec et al., 2000***; ***Gui et al., 2006***). Furthermore, we found that Pyk2 co-immunoprecipitated with $Ca_V1.2$ in parallel to Src. We identified the loop between domains two and three of $\alpha_1 1.2$ as the Pyk2-binding site. Stimulation of PKC either directly with PMA or through the G_q-coupled bradykinin (BK) receptor leads to tyrosine phosphorylation of $\alpha_1 1.2$ in PC12 cells. Abrogation of Pyk2 or Src activity ablated the phosphorylation. Finally, we discovered that the LTP in young mice mediated by LTCC-dependent Ca^{2+} influx during 200 Hz tetani (termed LTP_{LTCC}) that is not NMDAR dependent, required α_1AR stimulation and both Pyk2 and Src activity. These findings implicate upregulation of $Ca_V1.2$ activity by α_1AR–Pyk2–Src signaling as a critical process for control of synaptic strength. Our findings indicate that $Ca_V1.2$ forms a supramolecular signaling complex (signalosome) with PKC, Pyk2, and Src and that α_1AR–PKC–Src–$Ca_V1.2$ signaling constitutes a central regulatory mechanism of neuronal activity and synaptic plasticity by NE.

Results

α_1AR signaling augments LTCC activity in hippocampal neurons via PKC, Pyk2, and Src

We performed cell-attached recordings from cultured hippocampal neurons for single-channel analysis, which allows pharmacological isolation of LTCCs by application of ω-conotoxins GVIA and MVIIC (***Hall et al., 2013***; ***Oliveria et al., 2007***; ***Patriarchi et al., 2016***; ***Qian et al., 2017***). LTCC channel activity was measured by cell-attached recordings, which yielded the product of the number of channels (N) and the open probability (Po) of each single channel. Application of phenylephrine (PHE), a selective agonist for all three α_1ARs, augmented N × Po of LTCCs from 0.18 ± 0.0433 (H_2O vehicle Control, $n = 11$) to 0.6156 ± 0.1386 (PHE; $n = 13$, $p \leq 0.01$; ***Figure 1A–C***). This increase was blocked by the selective α_1AR antagonist prazosin (0.2954 ± 0.0607; $n = 10$, $p \leq 0.05$), indicating that PHE acted through α_1ARs and not other G-protein-coupled receptors. Prazosin by itself had no effect, vs. vehicle control (0.1846 ± 0.04624; $n = 10$) suggesting that there is little if any regulation of LTCCs under basal conditions in neurons by α_1ARs. PHE also increased the peak current of the ensemble average current in a prazosin-sensitive manner (***Figure 1D, E***).

Because direct phosphorylation of $\alpha_1 1.2$ by PKC inhibits $Ca_V1.2$ activity in heart (***McHugh et al., 2000***), we explored whether PKC might upregulate $Ca_V1.2$ activity indirectly via other kinases. PKC can activate Pyk2 (***Bartos et al., 2010***; ***Dikic et al., 1996***; ***Huang et al., 2001***; ***Lev et al., 1995***) and thereby Src (***Dikic et al., 1996***; ***Huang et al., 2001***). Src, in turn, augments LTCC activity (***Bence-Hanulec et al., 2000***; ***Endoh, 2005***; ***Gui et al., 2006***; ***Hu et al., 1998***; ***Strauss et al., 1997***; ***Wu et al., 2001***). Therefore, we tested whether block of Pyk2 and Src affects upregulation of LTCC activity by PHE. In a new set of recordings augmentation of LTCC activity by PHE from NPo of 0.2008 ± 0.03348 (dimethyl sulfoxide (DMSO) vehicle control, $n = 33$) to 0.3272 ± 0.04412 (PHE, $n = 33$; $p \leq 0.01$; ***Figure 2A–C***) was completely blocked by two different PKC inhibitors, bisindolylmaleimide I (GF109203X; Bis I; 0.1412 ± 0.03305; $n = 11$, $p \leq 0.01$) and chelerythrine (Chel; 0.05801 ± 0.01508; $n = 12$, $p \leq 0.001$), the Pyk2-selective inhibitor PF-719 (0.09118 ± 0.02828; $n = 10$, $p \leq 0.01$) and two structurally different Src family kinase inhibitors, PP2 (0.01487 ± 0.006808; $n = 7$, $p \leq 0.001$) and SU6656 (0.09149 ± 0.02866; $n = 9$, $p \leq 0.01$). Peak currents of ensemble averages showed respective changes (***Figure 2D, E***). Accordingly, α_1AR signaling increases LTCC activity via a PKC–Pyk2–Src signaling cascade. Notably, stimulation of two other major G_q-protein-coupled receptors in neurons, that is, the metabotropic mGluR1/5 receptors with dihydroxyphenylglycine (DHPG) and muscarinic receptors with muscarine, did not significantly increase LTCC activity, although there was a tendency for DHPG to do so (***Figure 2—figure supplement 1***).

PKC augments LTCC activity in hippocampal neurons via Pyk2 and Src

To further establish a role of Pyk2 and Src, we directly stimulated PKC by including PMA in the bath solution during single-channel recording of LTCCs in hippocampal neurons. PMA increased NPo of LTCCs by around twofold from 0.1099 ± 0.0173 (DMSO control, $n = 45$) to 0.232 ± 0.03269 (PMA, $n = 38$; $p \leq 0.001$, ***Figure 3A–C***). This increase was blocked by Pyk2 inhibitors PF-719 (NPo = 0.1407 ± 0.02705, $n = 13$, $p \leq 0.05$) and PF-431396 (NPo = 0.09282 ± 0.01765, $n = 18$, $p \leq 0.001$) and by Src inhibitors PP2 (NPo = 0.05614 ± 0.01815, $n = 14$, $p \leq 0.001$) and SU6656 (NPo = 0.02951 ± 0.00555,

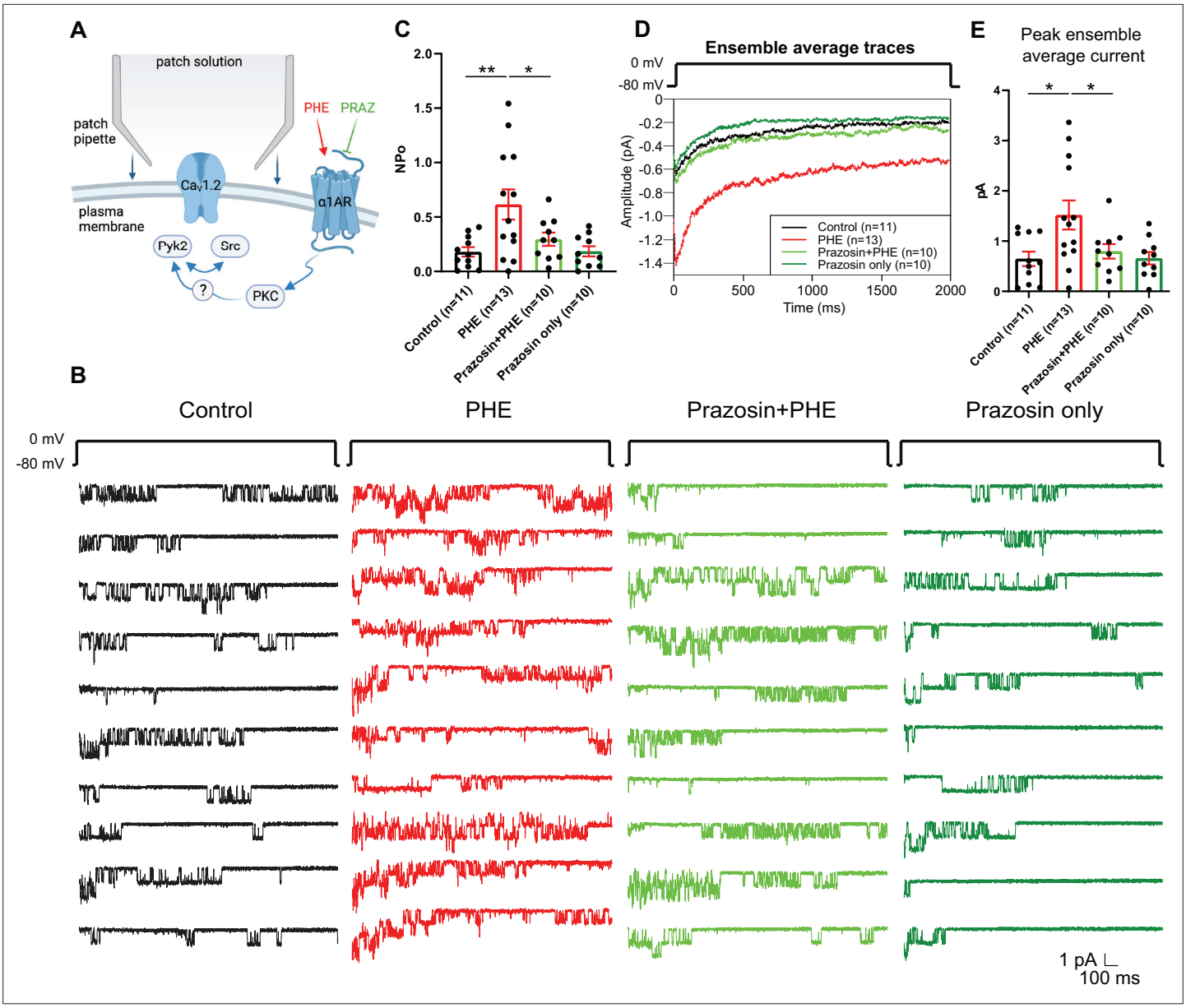

Figure 1. The α_1AR agonist phenylephrine (PHE) augments NPo of L-type Ca^{2+} channels (LTCCs) in hippocampal neurons. (**A**) Neurons were preincubated with vehicle, PHE and prazosin (PRAZ) before seal formation. (**B**) Ten consecutive traces from representative cell-attached single-channel recordings of LTCCs from cultured hippocampal neurons with vehicle (water; black), 10 µM PHE (red), PHE plus 20 nM prazosin (bright green), and prazosin alone (dark green). (**C**) The increase in NPo by PHE was blocked by prazosin. $F_{3,40}$ = 5.474. Control vs. PHE, p = 0.0036; PHE vs. Prazosin + PHE, p = 0.0334; Control vs. Prazosin only, p = 0.9723. (**D**) Ensemble averages during depolarization. (**E**) The increase in ensemble average peak currents by PHE was blocked by prazosin. $F_{3,40}$ = 4.506. Control vs. PHE, p = 0.0101; PHE vs. Prazosin + PHE, p = 0.0316; Control vs. Prazosin only, p = 0.9722. (**C, E**) Data are presented as means ± standard error of the mean (SEM). *n* represents the number of cells (*p ≤ 0.05, **p ≤ 0.01; analysis of variance [ANOVA] with post hoc Holm–Sidak's multiple comparisons test). Panel A was created using Biorender.com.

n = 8, p ≤ 0.001). Peak currents of ensemble averages showed respective changes (***Figure 3D, E***). The L-type calcium channel blocker isradipine completely blocked L-type currents in the presence of PMA, indicating successful isolation of L-type single-channel currents (***Figure 3—figure supplement 1***). These results show that in hippocampal neurons, PKC activation stimulates LTCC activity and this augmentation requires Pyk2 and Src activity.

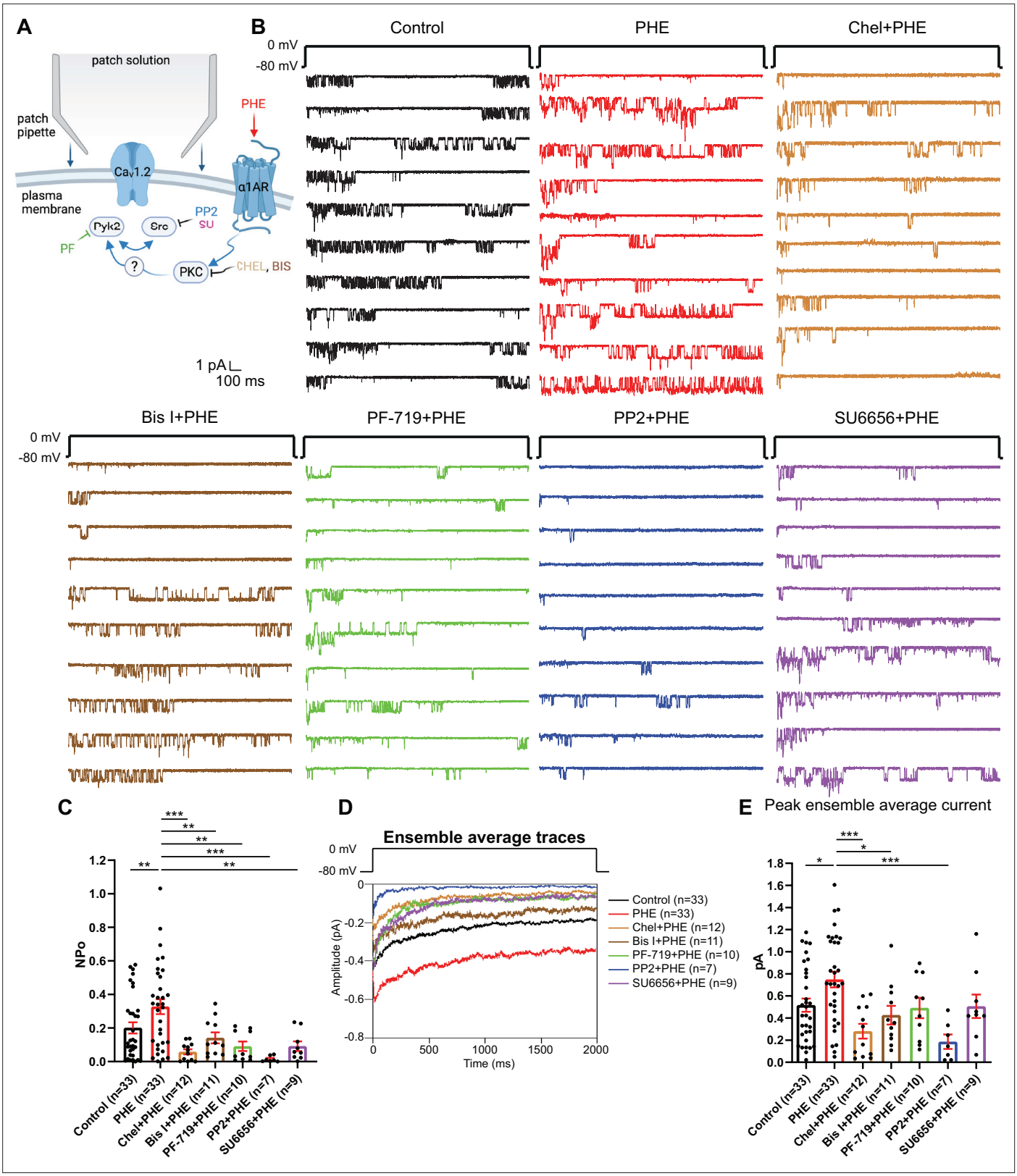

Figure 2. The phenylephrine (PHE)-induced increase in NPo of L-type Ca^{2+} channels (LTCCs) in hippocampal neurons requires PKC, Pyk2, and Src. (**A**) Neurons were preincubated with vehicle, PHE, and the indicated kinase inhibitors before seal formation. (**B**) Ten consecutive traces from representative cell-attached single-channel recordings of LTCCs with vehicle (0.1% DMSO; black) and PHE either alone (red) or with the PKC inhibitors chelerythrine (Chel; 10 μM; bright brown) and bisindolylmaleimide I (Bis I; 100 nM; dark brown), the Pyk2 inhibitor PF-719 (1 μM; green), or the Src inhibitors PP2

Figure 2 continued on next page

Figure 2 continued

(10 μM; blue) and SU6656 (10 μM; purple). (**C**) The increase in NPo by PHE was blocked by all inhibitors. $F_{6,108}$ = 6.434. Control vs. PHE, p = 0.0076; PHE vs. Chel + PHE, p = 0.0001; PHE vs. Bis I + PHE, p = 0.0076; PHE vs. PF-719 + PHE, p = 0.0018; PHE vs. PP2 + PHE, p = 0.0003; PHE vs. SU6656 + PHE, p = 0.0022. (**D**) Ensemble averages during depolarization. (**E**) The increase in ensemble average peak currents by PHE was blocked by PKC inhibitors chelerythrine, bisinolylmaleimide I, and Src inhibitor PP2. $F_{6,108}$ = 4.839. Control vs. PHE, p = 0.0242; PHE vs. Chel + PHE, p = 0.0004; PHE vs. Bis I + PHE, p = 0.0242; PHE vs. PF-719 + PHE, p = 0.0723; PHE vs. PP2 + PHE, p = 0.0006; PHE vs. SU6656 + PHE, p = 0.0723. (**C, E**) Data are presented as means ± standard error of the mean (SEM). *n* represents the number of cells (*p ≤ 0.05, **p ≤ 0.01, ***p ≤ 0.001; analysis of variance [ANOVA] with post hoc Holm–Sidak's multiple comparisons test). Panel A was created using Biorender.com.

The online version of this article includes the following figure supplement(s) for figure 2:

Figure supplement 1. Group I mGluR and muscarinic receptor agonists did not change NPo of L-type Ca^{2+} channels (LTCCs) in hippocampal neurons.

α_1AR signaling augments single-channel open probability Po of LTCCs in neurons

Preincubation of neurons with PHE could promote either surface insertion or Po of LTCCs. To test whether PHE augmented specifically Po, we used pipettes with smaller diameters to minimize patch size and channel number in the patch, as reflected by pipette resistences of 7–12 vs. 3.5–5.5 MΩ in the preceding experiments. This approach typically resulted in <4 channels per patch, allowing exact determination of channel number and thereby calculation of single-channel Po. PHE was acutely washed on after establishing baseline activity to avoid delays as occurring when recording the effect of preincubation of neurons with PHE during which new channels could have been inserted (***Figure 4A***). PHE consistently increased within 2–3 min Po and peak currents as determined by ensemble averages (***Figure 4B–D***).

Application of the endogenous agonist NE to the outside of the cell-attached pipette was equally able to augment single-channel Po and peak currents of ensemble averages (***Figure 4E–G***). Of note, the β_2AR-selective adrenergic agonist albuterol can also augment Po of $Ca_V1.2$ by stimulating the $Ca_V1.2$-associated β_2AR, adenylyl cyclase and PKA (***Davare et al., 2001***; ***Dittmer et al., 2014***; ***Murphy et al., 2014***; ***Oliveria et al., 2007***; ***Patriarchi et al., 2016***; ***Qian et al., 2017***). However, it does so only when applied inside the patch pipette and not when applied after seal formation to the outside, reflective of highly localized, spatially restricted signaling events (***Davare et al., 2001***; ***Dittmer et al., 2014***; ***Murphy et al., 2014***; ***Oliveria et al., 2007***; ***Patriarchi et al., 2016***; ***Qian et al., 2017***). Accordingly, NE applied to the outside of the pipette augments Po not via β_2AR but rather via α_1AR signaling. Consistently, the increases in single-channel Po and peak currents of ensemble averages seen with NE were remarkably similar to the respective PHE effects.

To further test the role of α_1AR vs. β_2AR signaling in this recording configuration, we applied NE either alone or together with the α_1AR antagonist prazosin to the neurons before seal formation and recording of channel activity (***Figure 5A***). NE increased Po and peak current of ensemble averages more strongly in this approach than when applied only to the outside of the pipettes (***Figure 5B–D***). This effect was inhibited but not fully blocked when prazosin was co-applied with NE. These two effects are consistent with upregulation of $Ca_V1.2$ activity by NE via both α_1AR and β_2AR signaling.

BK augments Po of LTCCs in neurons

The above results indicate that signaling by the G_q-coupled α_1AR promotes LTCC activity in a manner that is spatially much less localized if at all as opposed to signaling by the G_s-coupled β_2AR. Stimulation of other prominent G_q-coupled receptors, mGluR and muscarinic receptors, yielded little or no effects, respectively, on LTCC activity (***Figure 2—figure supplement 1***), possibly because those might be to far removed from the LTCCs in soma where the recordings were performed. Another G_q-coupled receptor that is prominent in the hippocampus is the BK receptor 2 (BK2). Application of BK to the outside of the patch pipette after establishing baseline activity of LTCCs (***Figure 6A***) significantly augmented Po (***Figure 6B–D***). In this set of experiments, the identity of the Ca^{2+} channels in the patch was confirmed by applying the LTCC activity promoting Bay K8644, which, consistently, augmented the current under the patch.

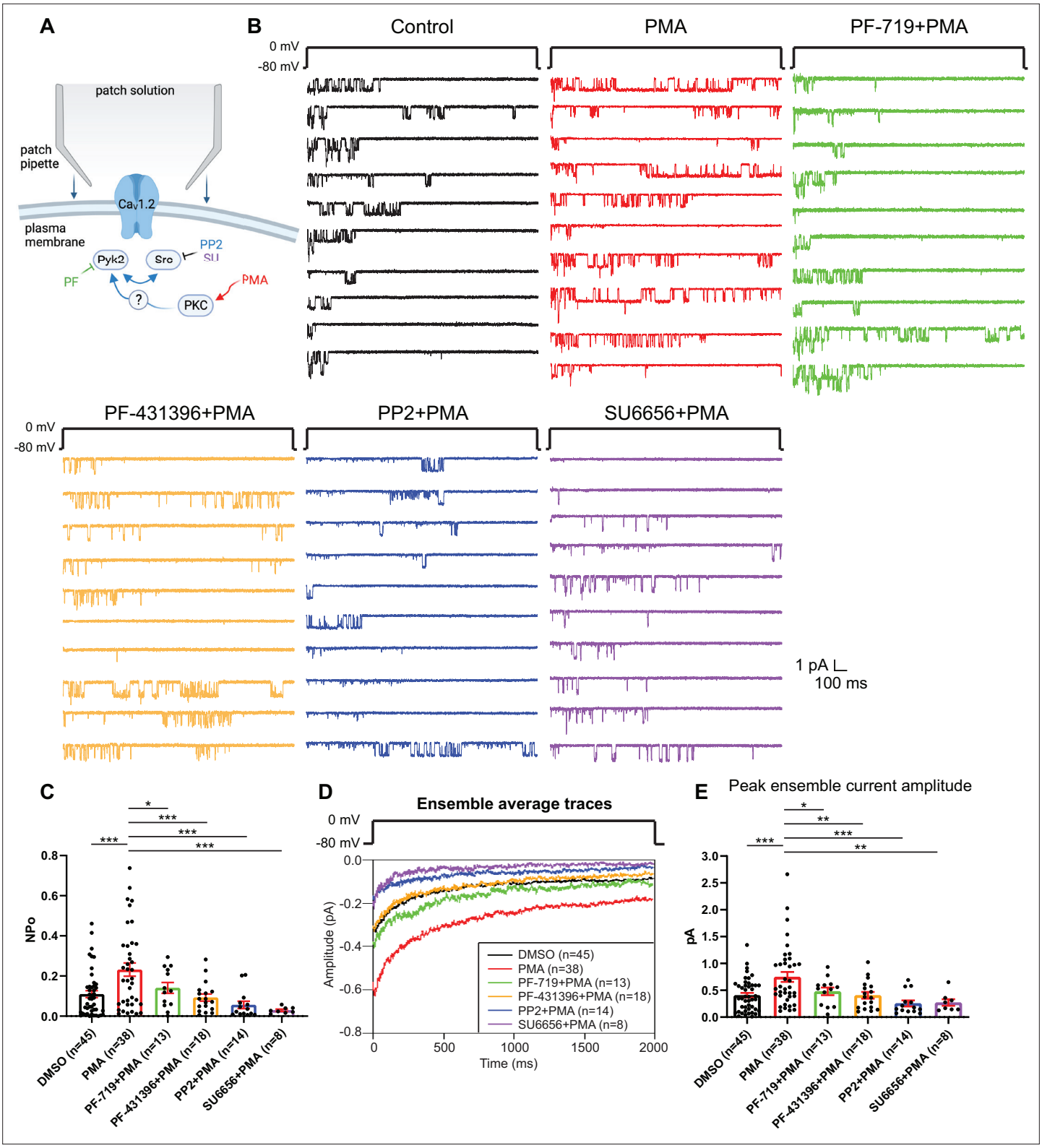

Figure 3. The increase in NPo of L-type Ca^{2+} channels (LTCCs) in hippocampal neurons by PKC requires Pyk2 and Src. (**A**) Neurons were preincubated with vehicle, the phorbol ester phorbol-12-myristate-13-acetate (PMA), and the indicated kinase inhibitors before seal formation. (**B**) Ten consecutive traces from representative cell-attached single-channel recordings of LTCCs with vehicle (0.06% DMSO; black) and 2 μM PMA either alone (red) or with the Pyk2 inhibitors PF-719 (1 μM; green) and PF-431396 (3 μM; orange), or the Src inhibitors PP2 (10 μM; blue) and SU6656 (10 μM; purple). (**C**) The increase in NPo by PMA was blocked by all inhibitors. $F_{5,130}$ = 6.530. DMSO vs. PMA, p = 0.0003; PMA vs. PF-719 + PMA, p = 0.0372, PMA vs. PF-431396

Figure 3 continued on next page

Figure 3 continued

+ PMA, p = 0.0009; PMA vs. PP2 + PMA, p = 0.0003; PMA vs. SU6656 + PMA, p = 0.0005. (**D**) Ensemble averages during depolarization. (**E**) The increase in ensemble average peak currents by PMA was blocked by all inhibitors. $F_{5,130}$ = 5.665. DMSO vs. PMA, p = 0.0003; PMA vs. PF-719 + PMA, p = 0.0303, PMA vs. PF-431396 + PMA, p = 0.0051; PMA vs. PP2 + PMA, p = 0.0003; PMA vs. SU6656 + PMA, p = 0.0051. (**C, E**) Data are presented as means ± standard error of the mean (SEM). *n* represents the number of cells (*p ≤ 0.05, **p ≤ 0.01, ***p ≤ 0.001; analysis of variance [ANOVA] with post hoc Holm–Sidak's multiple comparisons test). Panel A was created using Biorender.com.

The online version of this article includes the following figure supplement(s) for figure 3:

Figure supplement 1. L-type channel blocker isradipine completely blocks L-type single-channel currents in the presence of phorbol-12-myristate-13-acetate (PMA).

Pyk2 co-immunoprecipitates with $Ca_V1.2$ from brain and heart

Kinases and proteins that regulate kinase activity are often found in complexes with their ultimate target proteins (i.e., their ultimate substrates) including different ion channels for efficient and specific signaling (***Dai et al., 2009***; ***Dodge-Kafka et al., 2006***). Both, PKC (***Navedo et al., 2008***; ***Yang et al., 2005***) and Src (***Bence-Hanulec et al., 2000***; ***Chao et al., 2011***; ***Hu et al., 1998***), are associated with $Ca_V1.2$. We tested in brain and heart (where $Ca_V1.2$ is most abundant) whether the same is true for

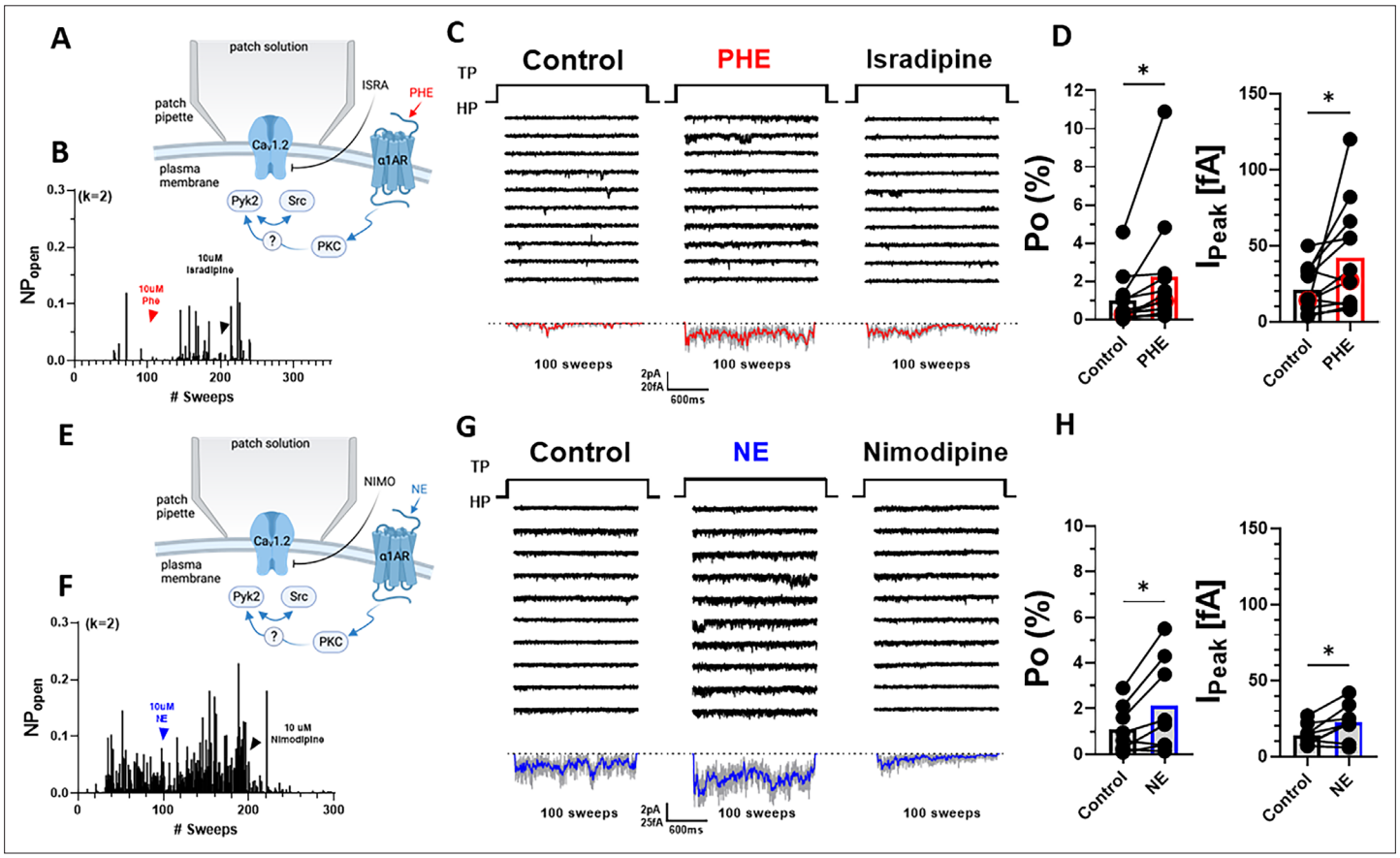

Figure 4. α_1AR signaling augments Po of L-type Ca^{2+} channels (LTCCs) in hippocampal neurons. (**A, E**) Seals were formed by the recording pipettes before application of phenylephrine (PHE) or norepinephrine (NE) and ultimately of either isradipine or nimodipine to ensure channel activity was mediated by LTCCs. (**B**) Sample diary shows time course of Po before and after application of 10 µM PHE and then 10 µM isradipine. The number of channels under the patch was estimated based on the maximal number of observed stagged openings in each patch (*k*; upper left). (**C**) Ten consecutive traces from representative cell-attached single-channel LTTC recordings before and after application of PHE and then isradipine. Bottom panels show ensemble averages. (**D**) PHE increases Po (left) and peak currents of ensemble averages (*n* = 12 cells; right). (**F**) Sample diary shows time course of Po before and after application of 10 µM NE and then 10 µM isradipine. (**G**) Ten consecutive traces from representative cell-attached single-channel recordings of LTCCs before and after application of NE and then nimodipine. Bottom panels show ensemble averages. (**H**) NE increases Po (left) and peak currents of ensemble averages (*n* = 8 cells; right). (**D, H**) Data are presented as means ± standard error of the mean (SEM). Statistical significance was tested by a paired, two-tailed Student's *t*-test, *p ≤ 0.05. Panels A and E were created using Biorender.com.

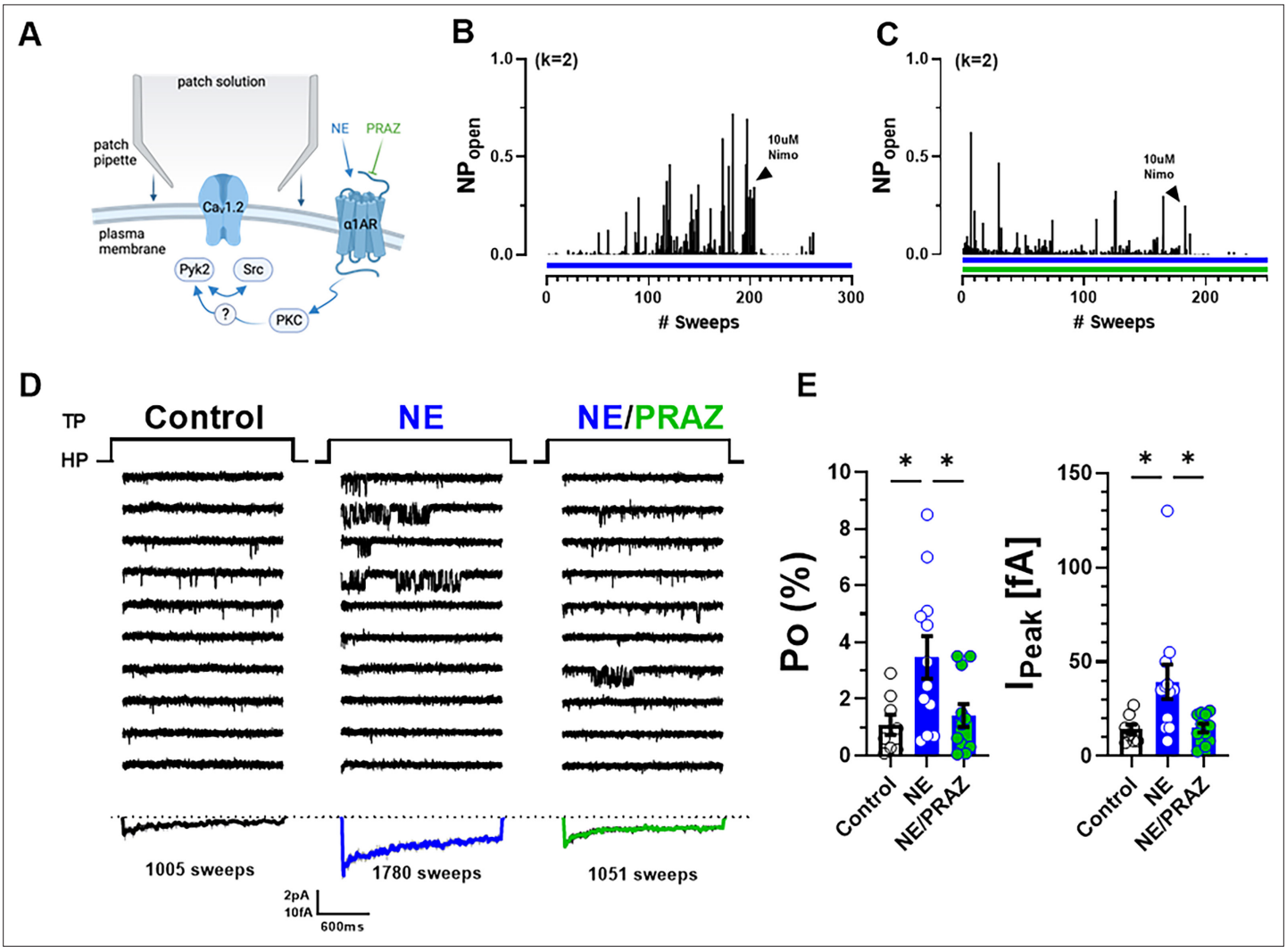

Figure 5. Norepinephrine (NE) can augment Po of L-type Ca^{2+} channels (LTCCs) via α_1AR signaling in hippocampal neurons. (**A**) Neurons were preincubated with NE ± prazosin (PRAZ) before seal formation. (**B, C**) Sample diaries show time courses of Po recordings obtained after preincubation with either NE alone or NE + PRAZ and seal formation. The number of channels under the patch was estimated based on the maximal number of observed stagged openings in each patch (*k*; upper left). (**D**) Ten consecutive traces from representative cell-attached single-channel recordings of LTCCs under control conditions or upon pre-incubation with either NE alone or NE plus PRAZ. Bottom panels show ensemble averages. (**E**) NE strongly increases Po (left) and peak currents of ensemble averages (right), which was strongly but not fully inhibited by PRAZ. Data are presented as means ± standard error of the mean (SEM; Control, *n* = 8 cells; NE, *n* = 12 cells; NE/PRAZ, *n* = 11 cells). Statistical significance was tested by a one-way analysis of variance (ANOVA) with Bonferroni correction, *p ≤ 0.05. Panel A was created using Biorender.com.

Pyk2. The Pyk2 antibody detected a single immunoreactive band with an apparent M_R of ~120 kDa in brain lysate (***Figure 7A***) and two bands in the same range in heart (***Figure 7A, B***), as reported earlier (***Dikic et al., 1998***). The shorter form is missing 42 residues in the proline-rich region of Pyk2, which affects its binding selectivity to proteins with SH3 domains. The single size form of Pyk2 present in brain and its two size forms expressed in heart co-immunoprecipitated with $Ca_V1.2$ (***Figure 7A, B***). No Pyk2 immunoreactive band was detectable when the immunoprecipitation (IP) was performed with control IgG, demonstrating that the co-IP of Pyk2 with $Ca_V1.2$ was specific. The detergent extracts from brain and heart were cleared of non-soluble material by ultracentrifugation prior to co-IP of Pyk2 with $Ca_V1.2$. Thus, our findings indicate that Pyk2 forms a bona fide protein complex with $Ca_V1.2$ rather than just co-residing in a detergent-resistant subcellular compartment. We also confirmed earlier work (***Figure 7A***, bottom panel) that indicated association of Src with $Ca_V1.2$ in vitro (***Bence-Hanulec et al., 2000***; ***Endoh, 2005***; ***Gui et al., 2006***; ***Hu et al., 1998***; ***Strauss et al., 1997***; ***Wu et al., 2001***) and in intact cells (***Bence-Hanulec et al., 2000***; ***Chao et al., 2011***; ***Hu et al., 1998***).

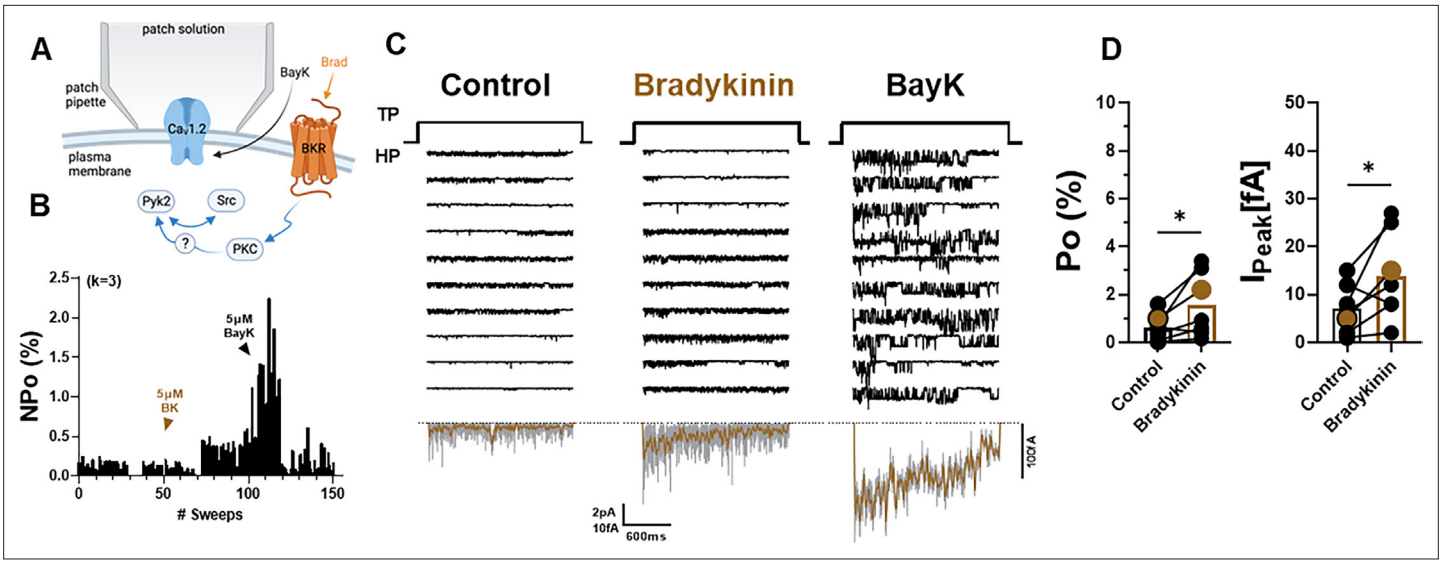

Figure 6. Bradykinin (BK) signaling augments Po of L-type Ca^{2+} channels (LTCCs) in hippocampal neurons. (**A**) Seals were formed by the recording pipettes before application of BK and ultimately of BayK8644 (BayK) to ensure channel activity was mediated by LTCCs. (**B**) Sample diary shows time course of Po before and after application of 5 µM BK and then 5 µM BayK to not only provide further evidence that the channels in the patch were LTCC but also aid in determining channel number *k* (upper left), which is the number of channels under the patch as estimated based on the maximal number of observed stagged openings in each patch. (**C**) Ten consecutive traces from representative cell-attached single-channel recordings of LTCCs before and after application of BK and then BayK. Bottom panels show ensemble averages. (**D**) BK increases Po (left) and peak currents of ensemble averages (right). Data are presented as means ± standard error of the mean (SEM; $n = 7$ cells). Statistical significance was tested by a paired, two-tailed Students *t*-test, *p ≤ 0.05. Panel A was created using Biorender.com.

Pyk2 binds to the loop between domains II and III of $\alpha_1$1.2

To further confirm a direct interaction between Pyk2 and Ca_V1.2 we performed pulldown experiments using purified solubilized His-tagged Pyk2 and purified bead-bound GST-tagged $\alpha_1$1.2 fragments covering all intracellular regions of $\alpha_1$1.2 (***Supplementary file 1***, ***Snutch et al., 1990***). As demonstrated earlier, all $\alpha_1$1.2 fragments were present in comparable amounts (***Hall et al., 2013***; ***Patriarchi et al., 2016***). The GST fusion protein covering the loop between domains II and III of $\alpha_1$1.2 specifically pulled down Pyk2 (***Figure 7C, D***) indicating that Pyk2 directly binds to this region of the α_1 subunit.

Inhibitors of Pyk2 and Src block the increase in $\alpha_1$1.2 tyrosine phosphorylation upon stimulation of PKC

PC12 cells are of neural-endocrine crest origin and widely used as model cells for neuronal signaling and development. They express high levels of Ca_V1.2 (***Eiki et al., 2009***; ***Mustafa et al., 2010***; ***Taylor et al., 2000***; ***Walter et al., 2000***), the BK receptor, and Pyk2 (***Bartos et al., 2010***; ***Dikic et al., 1996***; ***Lev et al., 1995***), making them an ideal model system for the difficult biochemical analysis of Ca_V1.2 phosphorylation. To characterize tyrosine phosphorylation of $\alpha_1$1.2 we performed IP with the general anti-phosphotyrosine antibody 4G10 (***Clifton et al., 2004***; ***Ward et al., 1992***). For this purpose, lysates were extracted with 1% sodium dodecyl sulfate (SDS) at 65°C followed by neutralization of SDS and ultracentrifugation before IP with the general anti-phosphotyrosine antibody 4G10 (***Clifton et al., 2004***; ***Ward et al., 1992***). IP with 4G10 followed by immunoblotting (IB) with antibodies against the protein of interest is more reliable and more broadly applicable than the inverse. Because $\alpha_1$1.2 does not re-associate with its binding partners after complex dissociation with SDS and the neutralization and dilution of SDS with Triton X-100 (***Davare et al., 1999***; ***Hell et al., 1995***; ***Hell et al., 1993b***; see also ***Leonard and Hell, 1997***), detection of $\alpha_1$1.2 by IB in the 4G10 IP would reflect specific tyrosine phosphorylation of the $\alpha_1$1.2 subunit and not its artefactual re-association with an $\alpha_1$1.2-associating tyrosine-phosphorylated protein that had been pulled down by the 4G10 antibody. This approach also allows analysis of tyrosine phosphorylation of Pyk2 within the same sample.

PC12 cells were pretreated with vehicle (0.02% DMSO), the Pyk2 inhibitor PF-431396, or the Src inhibitors SU6656 and PP2 or its inactive analogue PP3 for 5 min before application of BK or PMA for

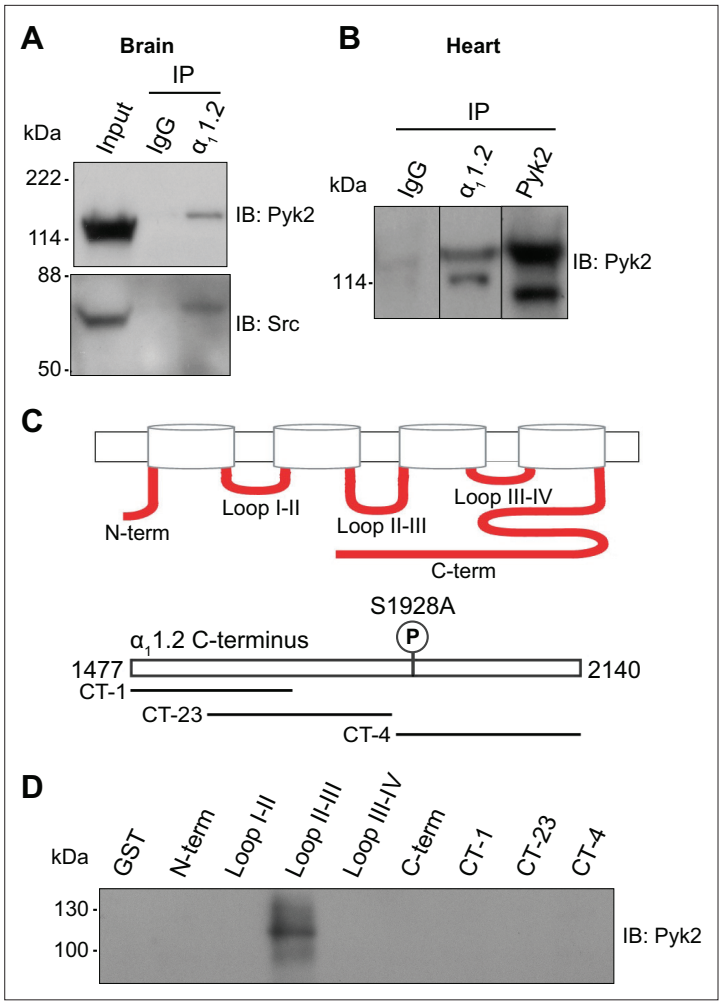

Figure 7. Pyk2 binds to the loop between domains II and III of $\alpha_1$1.2. Co-immunoprecipitation of Pyk2 and Src with Ca_V1.2 from brain (**A**) and heart (**B**). Triton X-100 extracts were cleared from non-soluble material by ultracentrifugation before immunoprecipitation (IP) with antibodies against $\alpha_1$1.2, Pyk2 itself, or non-immune control antibodies (rabbit IgG) and immunoblotting (IB) with anti-Pyk2 and anti-Src. Brain lysate (**A**, Input; 20 µl) and Pyk2 immunoprecipitates (**B**) served as positive control for detection of Pyk2 and Src by IB. Lanes for rabbit IgG control and $\alpha_1$1.2 IP in B are from the same IB as the Pyk2 IP, which is depicted from a shorter exposure than the IgG and $\alpha_1$1.2 IP lanes because IB signal was much stronger after Pyk2 IP than $\alpha_1$1.2 IP. Comparable results were obtained in four independent experiments. (**C**) Schematic diagram of the intracellular $\alpha_1$1.2 fragments used in the pulldown assay (***Supplementary file 1***). (**D**) Pulldown assay of Pyk2 binding to $\alpha_1$1.2 fragments. GST fusion proteins of the N-terminus, the loops between domains I and II, II and III, III and IV, the whole C-terminus, and three different overlapping fragments covering the C-terminus were expressed in *Escherichia coli*, immobilized on glutathione Sepharose, washed and incubated with purified His-tagged Pyk2. Comparable amounts of fusion proteins were present (data not shown but see ***Hall et al., 2013***; ***Hall et al., 2007***; ***Patriarchi et al., 2016***; ***Xu et al., 2010***). Comparable results were obtained in five independent experiments.

The online version of this article includes the following source data for figure 7:

Source data 1. Original files of the full raw unedited blots with bands labeled in red boxes.

10 min. BK strongly activates Pyk2 in PC12 cells via its G_q-coupled cognate receptor (***Dikic et al., 1996***; ***Lev et al., 1995***). Using the 4G10 IP method, we found that both PMA and BK increased tyrosine phosphorylation of Pyk2 as previously described (***Dikic et al., 1996***; ***Lev et al., 1995***; ***Figure 8A–C***). This increase was prevented by PF-431396. In parallel, we determined phosphorylation of Pyk2 on Y402 and Y579 by direct IB of PC12 lysates with corresponding phosphospecific antibodies. Upon stimulation via PKC, Pyk2 phosphorylates itself in trans on Y402 (***Bartos et al., 2010***; ***Park et al., 2004***) and then binds with phosphoY402 to the SH2 domain of Src (***Dikic et al., 1996***). This binding

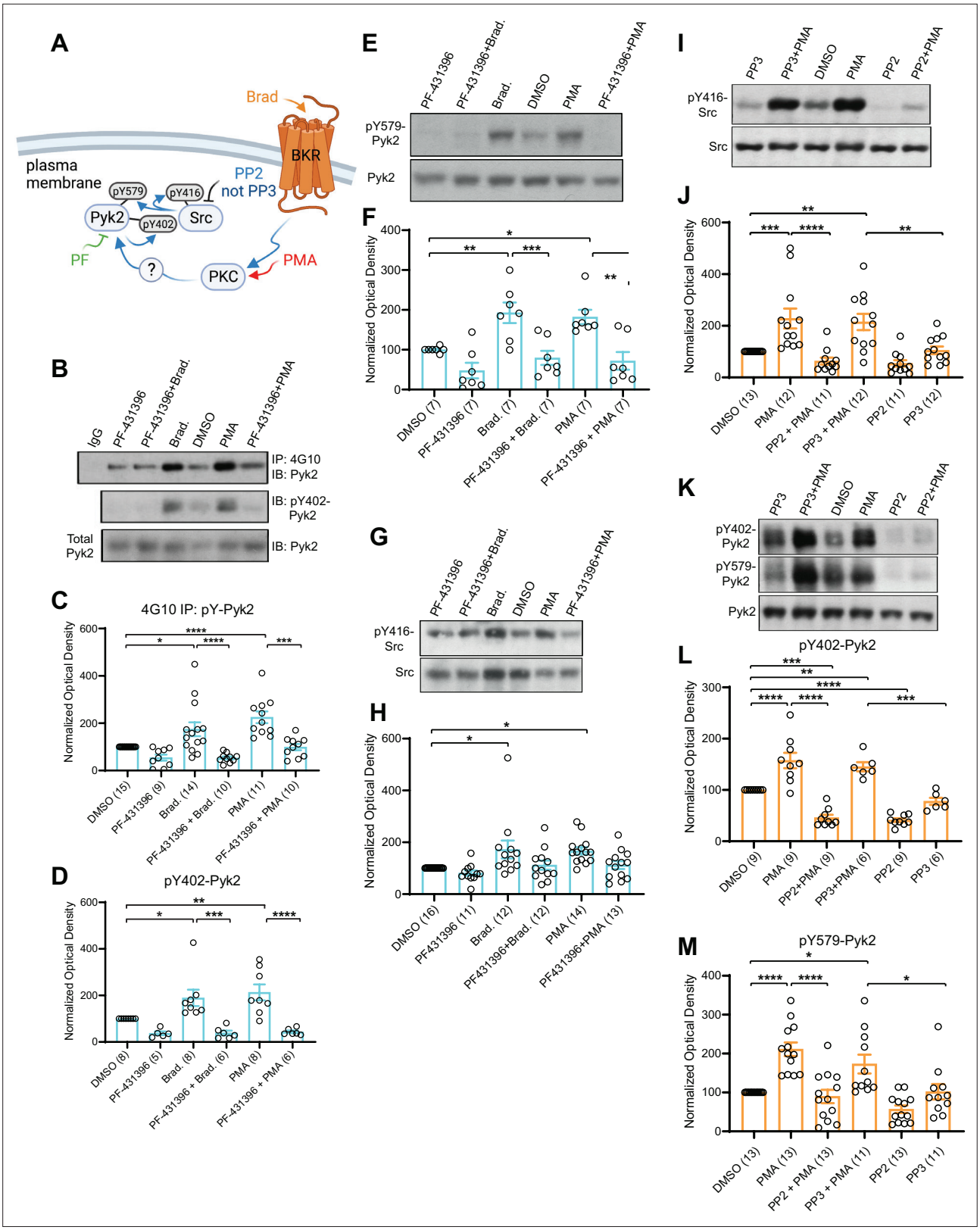

Figure 8. PKC activates interdependent Pyk2 and Src. PC12 cells were pretreated with vehicle (0.02% DMSO), the Pyk2 inhibitor PF-431396 (3 μM), and the Src inhibitor PP2 (10 μM) or its inactive analogue PP3 (10 μM) for 5 min before application of bradykinin (Brad., 2 μM) or phorbol-12-myristate-13-acetate (PMA, 2 μM) for 10 min, extraction with 1% sodium dodecyl sulfate (SDS) at 65°C to ensure dissociation of all proteins, neutralization of SDS with excess of Triton X-100, and ultracentrifugation. Supernatants were analysed by direct immunoblotting (IB) with the indicated Pyk2 and Src antibodies.

Figure 8 continued on next page

Figure 8 continued

Some samples underwent immunoprecipitation (IP) with the anti-phosphotyrosine antibody 4G10 before IB with anti-Pyk2 antibody (top panel in **A** and quantification in **B**). IgG indicates control IP with non-immune mouse IgG. (**A**) Schematic diagram depicting the bradykinin receptor–PKC–Pyk2/Src signaling cascade and drugs used to target each molecular entity. (**B**) Upper panel: Total pY levels of Pyk2 determined by IP with 4G10 and IB with anti-Pyk2. Middle panel: pY402 levels of Pyk2 detected with anti-pY402 in corresponding lysates. Lower panel: Levels of total Pyk2 detected with anti-Pyk2 in same lysates. (**C**) Ratios of total pY of Pyk2 after 4G10 IP to total Pyk2 in lysates, normalized to control. $F_{5,63}$ = 12.73. DMSO vs. Brad., p = 0.012; DMSO vs. PMA, p < 0.0001; Brad. vs. PF-431396 + Brad., p < 0.0001; PMA vs. PF-431396 + PMA, p = 0.0001. (**D**) Ratios of pY402 to total Pyk2 signals in lysates, normalized to control. $F_{5,35}$ = 10.94. DMSO vs. Brad., p = 0.039; DMSO vs. PMA, p = 0.0052; Brad. vs. PF-431396 + Brad., p = 0.0005; PMA vs. PF-431396 + PMA, p < 0.0001. (**E**) Upper panel: pY579 levels of Pyk2 detected with anti-pY579. Lower panel: Levels of total Pyk2 detected with anti-Pyk2 in same lysates. (**F**) Ratios of pY579 to total Pyk2 signals in lysates, normalized to control. $F_{5,36}$ = 10.18. DMSO vs. Brad., p = 0.0072; DMSO vs. PMA, p = 0.021; Brad. vs. PF-431396 + Brad., p = 0.0008; PMA vs. PF-431396 + PMA, p = 0.0011. (**G, I**) Upper panels: pY416 levels of Src detected with anti-pY416. Lower panels: Levels of total Src detected with anti-Src in same lysates. (**H, J**) Ratios of pY416 to total Src signals in lysates, normalized to control. (**H**) $F_{5,72}$ = 4.464. DMSO vs. Brad., p = 0.0167; DMSO vs. PMA, p = 0.0226. (**J**) $F_{5,65}$ = 11.06. DMSO vs. PMA, p = 0.001; PMA vs. PP2 + PMA, p < 0.0001; DMSO vs. PP3 + PMA, p = 0.0042; PP3 vs. PP3 + PMA, p = 0.0086. (**K**) Upper panel: pY402 levels of Pyk2 detected with anti-pY402. Middle panel: pY579 levels of Pyk2 detected with anti-pY579. Lower panel: Levels of total Pyk2 detected with anti-Pyk2 in same lysates. (**L, M**) Ratios of pY402 and pY579 to total Pyk2 signals in lysates, normalized to control. (**L**) $F_{5,42}$ = 35.85. DMSO vs. PMA, p < 0.0001; PMA vs. PP2 + PMA, p < 0.0001; PP3 vs. PP3 + PMA, p = 0.0001; DMSO vs. PP3 + PMA, p = 0.0068; DMSO vs. PP2 + PMA, p = 0.0001; DMSO vs. PP2, p < 0.0001. (**M**) $F_{5,68}$ = 13.40. DMSO vs. PMA, p < 0.0001; PMA vs. PP2 + PMA, p < 0.0001; PP3 vs. PP3 + PMA, p = 0.0362; DMSO vs. PP3 + PMA, p = 0.0202. (**C, D, F, H, J, L, M**) Data are presented as mean ± standard error of the mean (SEM). Number (*n*) of independent experiments for each condition are indicated inside bars. Statistical analysis was by analysis of variance (ANOVA) with post hoc Bonferroni's multiple comparisons test; *p ≤ 0.05, **p ≤ 0.01, ***p ≤ 0.001, ****p ≤ 0.0001. Bradykinin- and PMA-induced phosphorylation of Pyk2 on Y402 and Y579 and of Src on Y416, all of which were blocked by PF-431396 and PP2 but not the inactive PP3. Panel A was created using Biorender.com.

The online version of this article includes the following source data for figure 8:

Source data 1. Original files of the full raw unedited blots with bands labeled in red boxes.

stimulates Src (***Dikic et al., 1996***), which in turn phosphorylates Pyk2 on Y579 in its activation loop for full activation (***Avraham et al., 2000***; ***Figure 8A***). Src also phosphorylates itself in trans on Y416 in its activation loop for its own full activation (***Roskoski, 2015***), which was determined in parallel with a phosphospecific antibody. We found that BK and PMA increased phosphorylation of Pyk2 on Y402 (***Figure 8B–D***) and Y579 (***Figure 8E, F***) and of Src on Y416 (***Figure 8G, H***). PF-431396 blocked all of these phosphorylations indicating that Pyk2 acts downstream of PKC and upstream of Src. Furthermore, the Src inhibitor PP2, but not its inactive analog, PP3, also prevented PMA-induced Src autophosphorylation on Y416 (***Figure 8I, J***), as expected. Finally, PP2 inhibited PMA-induced phosphorylation of Pyk2 on Y402 and Y579 indicative of a self-maintaining positive feedback loop between Pyk2 and Src (***Figure 8K–M***). These results support the specific activation of both, Pyk2 and Src under our conditions and suggest that this activation occurs in a self-sustaining manner, which creates a quasi-molecular memory (***Figure 8A***).

Importantly, PMA and BK induced tyrosine phosphorylation of $\alpha_1$1.2 (***Figure 9***). This effect was blocked by the Pyk2 inhibitor PF-431396 (***Figure 9A–C***) and the Src inhibitors SU6656 and PP2, whereas the inactive PP2 analogue PP3 was without effect (***Figure 9D, E***). These data show that activation of PKC translates into tyrosine phosphorylation of $\alpha_1$1.2 and that this requires both Pyk2 and Src.

Knock down of Pyk2 and Src prevents the increase in $\alpha_1$1.2 tyrosine phosphorylation upon stimulation of PKC

To control for any potential side effects of PF-431396 and determine whether Pyk2 is required for PKC-induced tyrosine phosphorylation of $\alpha_1$1.2 we employed FIV and HIV lentiviral expression vectors for shRNAs targeting Pyk2 in PC12 cells. We first designed and cloned an shRNA-targeting rat Pyk2 (Sh1) into the FIV-based plasmid pVETL-GFP (***Bartos et al., 2010***; ***Boudreau and Davidson, 2012***; ***Harper et al., 2006***) and tested the ability and specificity of this construct to knockdown ectopically expressed Pyk2 in HEK293T/17 cells. Cells were co-transfected with vectors for expression of GFP-tagged rat Pyk2 (rPyk2-GFP) and the pVETL-Sh1-GFP or no shRNA control pVETL-GFP (***Figure 10A***) and Pyk2 expression levels in the transfected cell lysates were examined via IB. Expression of rPyk2-GFP was virtually abolished by pVETL-Sh1-GFP whereas the control pVETL-GFP had no effect (***Figure 10A***). IB with both tubulin and GAPDH antibodies confirmed that total protein levels were not affected by transfection of these plasmids (***Figure 10A***).

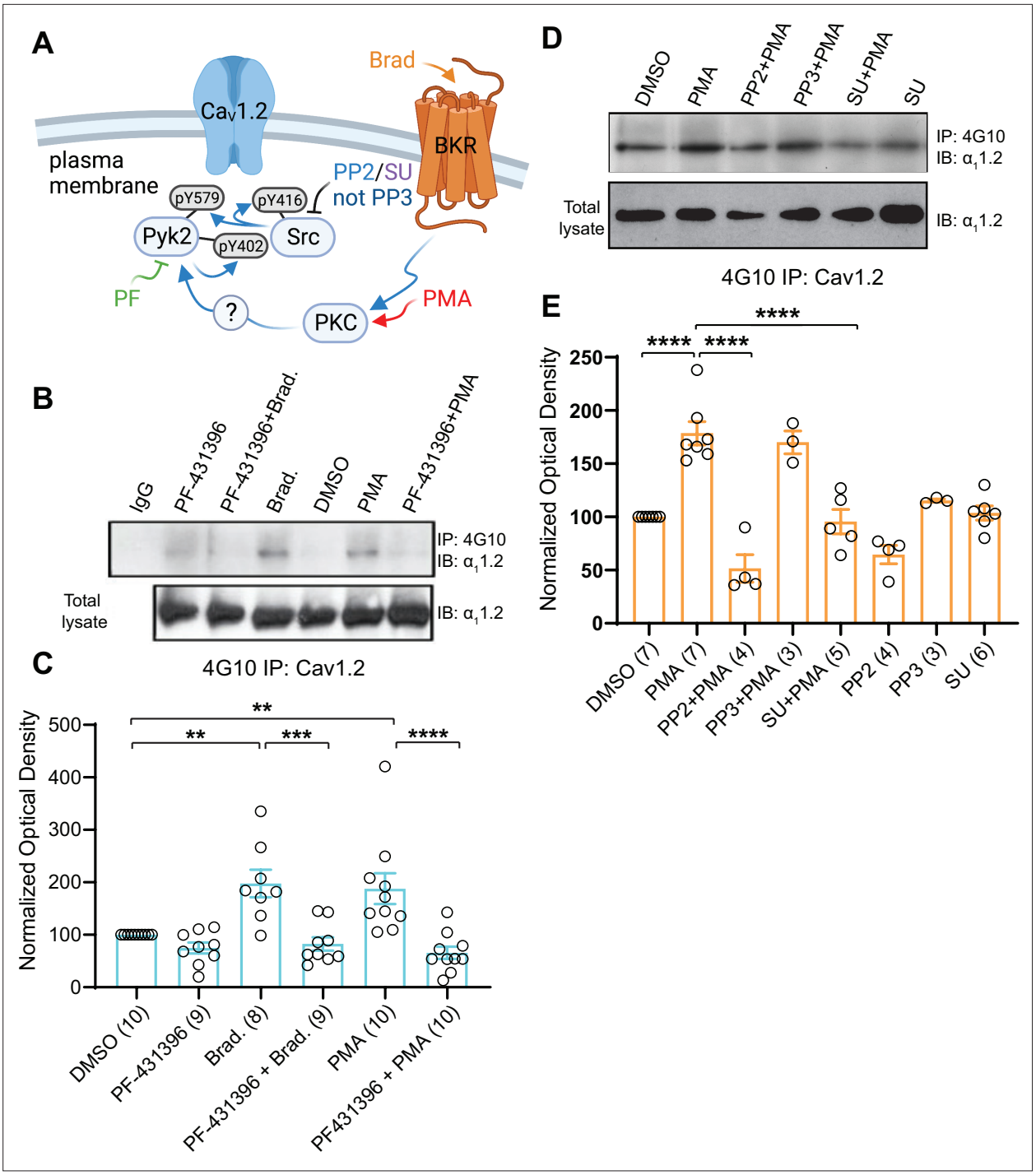

Figure 9. Increase in $\alpha_1$1.2 tyrosine phosphorylation by PKC is blocked by inhibitors or Pyk2 and Src. PC12 cells were treated as in ***Figure 8*** for analysis of tyrosine phosphorylation by immunoprecipitation (IP) with 4G10 and immunoblotting (IB) with anti-$\alpha_1$1.2. IgG indicates control IP with non-immune mouse IgG. Vehicle (0.02% DMSO), PF-431396 (3 μM), PP2 (10 μM), PP3 (10 μM), or SU6656 (SU, 10 μM) were applied 5 min before phorbol-12-myristate-13-acetate (PMA) or bradykinin (Brad.) when indicated. (**A**) Schematic diagram depicting the bradykinin receptor–PKC–Pyk2/Src–Ca_V1.2 signaling cascade and drugs used to target each molecular entity. (**B, D**) Upper panels: pY of $\alpha_1$1.2 determined by 4G10 IP and $\alpha_1$1.2 IB. Lower panels: Levels of total $\alpha_1$1.2 detected with anti-$\alpha_1$1.2 in corresponding lysates. (**C, E**) Ratios of pY signals in 4G10 IPs by IB with anti-$\alpha_1$1.2 to $\alpha_1$1.2 signals in lysates, normalized to control. Data are presented as mean ± standard error of the mean (SEM). Number (*n*) of independent experiments for each condition are indicated inside bars. Statistical analysis was by analysis of variance (ANOVA) with post hoc Bonferroni's multiple comparisons test. (**C**) $F_{5,50}$ = 10.65. DMSO vs. Brad., p = 0.0021; DMSO vs. PMA, p = 0.0036; Brad. vs. PF-431396 + Brad., p = 0.0003; PMA vs. PF-431396 + PMA, p < 0.0001. (**E**) $F_{7,31}$ = 23.67. DMSO vs. PMA, p < 0.0001; PMA vs. PP2 + PMA, p < 0.0001; PMA vs. SU + PMA, p < 0.0001 (**p ≤ 0.01, ***p ≤ 0.001, ****p ≤ 0.0001). Bradykinin- and

Figure 9 continued on next page

Figure 9 continued

PMA-induced $\alpha_1$1.2 tyrosine phosphorylation was blocked by PF-431396, SU6656 and PP2 but not the inactive PP3. Panel A was created using Biorender.com.

The online version of this article includes the following source data for figure 9:

Source data 1. Original files of the full raw unedited blots with bands labeled in red boxes.

Next we tested whether pVETL-Sh1-GFP would inhibit PMA- and BK-induced $\alpha_1$1.2 phosphorylation in PC12 cells. pVETL-Sh1-GFP lentiviral particles carrying the Sh1-shRNA and GFP expression cassettes were used to efficiently infect PC12 cells. Infected cells were monitored for GFP expression and then subjected to overnight serum starvation (to ensure low signaling levels) before treatment with PMA or BK. Fully SDS-dissociated tyrosine-phosphorylated proteins were immunoprecipitated with 4G10 before SDS–polyacrylamide gel electrophoresis (PAGE) and $\alpha_1$1.2 IB (***Figure 10B, C***). As before, PMA and BK induced in average an about 2.5-fold increase in tyrosine phosphorylation of the $\alpha_1$1.2 subunit, which was strongly repressed by Sh1 (***Figure 10B–D***). IB for total Pyk2 content confirmed Pyk2 knockdown by ~70–90% (***Figure 10B, C***, bottom panels). These findings indicate that depletion of Pyk2 potently blunts the PKC-mediated increase in $\alpha_1$1.2 tyrosine phosphorylation. Total $\alpha_1$1.2 content was not altered by Sh1. These findings indicate that Pyk2 knockdown does not affect $\alpha_1$1.2 expression levels and that the reduction in tyrosine-phosphorylated $\alpha_1$1.2 is likely not due to any potential off-target effects of the pVETL-Sh1-shRNA.

To further verify and extend these findings we obtained HIV-GFP lentiviral vectors for expression of validated unique 29mer shRNAs targeting Pyk2 (HIV-GFP-Pyk2ShA-D) and Src (HIV-GFP-SrcShA-D) as well as a scrambled, non-silencing control (HIV-GFP-Shscr). HIV-GFP-Pyk2ShB and C and HIV-GFP-SrcShB and C were most effective in knocking down endogenous Pyk2 and Src, respectively (***Figure 10E, F*** and data not shown). PC12 cells were transduced with HIV-GFP-Pyk2ShB and C and HIV-GFP-Shscr, serum starved, stimulated with PMA, harvested, and lysed before 4G10 IP and IB for $\alpha_1$1.2, Pyk2, Src, and tubulin. Total protein levels of $\alpha_1$1.2, Pyk2, Src, and tubulin in lysate were monitored in parallel. The Pyk2-targeting HIV-GFP-Pyk2ShB and C but not the scrambled control shRNA abrogated the PMA-induced increase in $\alpha_1$1.2 tyrosine phosphorylation (***Figure 10G***). Similarly, the Src-targeting HIV-GFP-SrcShB and C but not the scrambled control shRNA blocked the increase in $\alpha_1$1.2 tyrosine phosphorylation upon PMA application (***Figure 10G, H***). For quantification, phosphotyrosine signals were normalized to total $\alpha_1$1.2 in lysate (***Figure 10I***). None of the HIV viral constructs exhibited any detectable effects on protein expression of $\alpha_1$1.2, Pyk2, Src, or α-tubulin, vinculin, and GAPDH as determined in lysates suggesting these constructs did not affect general protein expression. Collectively, the above findings indicate that knockdown effects were specific and not simply the consequence of viral infection or expression of non-specific stem-loop RNAs. Taken together, our findings strongly support the hypothesis that PKC signaling mediates its effects on Ca_V1.2 through Pyk2 and Src.

Inhibition of Pyk2 and Src blocks LTCC-dependent LTP

Ca_V1.2 is concentrated in dendritic spines (***Hall et al., 2013***; ***Hell et al., 1996***; ***Leitch et al., 2009***) where it mediates Ca^{2+} influx (***Bloodgood and Sabatini, 2007***; ***Hoogland and Saggau, 2004***) and several forms of LTP (***Grover and Teyler, 1990***; ***Moosmang et al., 2005***; ***Patriarchi et al., 2016***; ***Qian et al., 2017***; ***Tigaret et al., 2021***). Notably, in older mice and rats, about half of the LTP (called LTP_{LTCC}) induced by four 200 Hz tetani, each 0.5 s long and 5 s apart, is insensitive to NMDAR blockade but abrogated by inhibition or elimination of Ca_V1.2 (***Boric et al., 2008***; ***Grover and Teyler, 1990***; ***Moosmang et al., 2005***; ***Shankar et al., 1998***; ***Wang et al., 2016***). Pharmacological inhibition and genetic disruption of Ca_V1.2 also abolish LTP induced by either pairing presynaptic stimulation with backpropagating action potentials (***Magee and Johnston, 1997***; ***Tigaret et al., 2021***; ***Tigaret et al., 2016***) or by 5 Hz/3 min tetani, the latter form of LTP requiring β_2AR signaling to upregulate Ca_V1.2 activity (***Patriarchi et al., 2016***; ***Qian et al., 2012***; ***Qian et al., 2017***). Thus, we hypothesized that upregulation of Ca_V1.2 activity by α_1AR signaling can augment LTCC-dependent forms of LTP.

LTP_{LTCC} is prominent in mice older than 1 year (30–40% above baseline) but small in mice younger than 3 months (10–15% above baseline) (***Boric et al., 2008***; ***Shankar et al., 1998***). LTP_{LTCC} requires Ca_V1.2 activity (***Moosmang et al., 2005***) and stimulation of PKC signaling via type I metabotropic

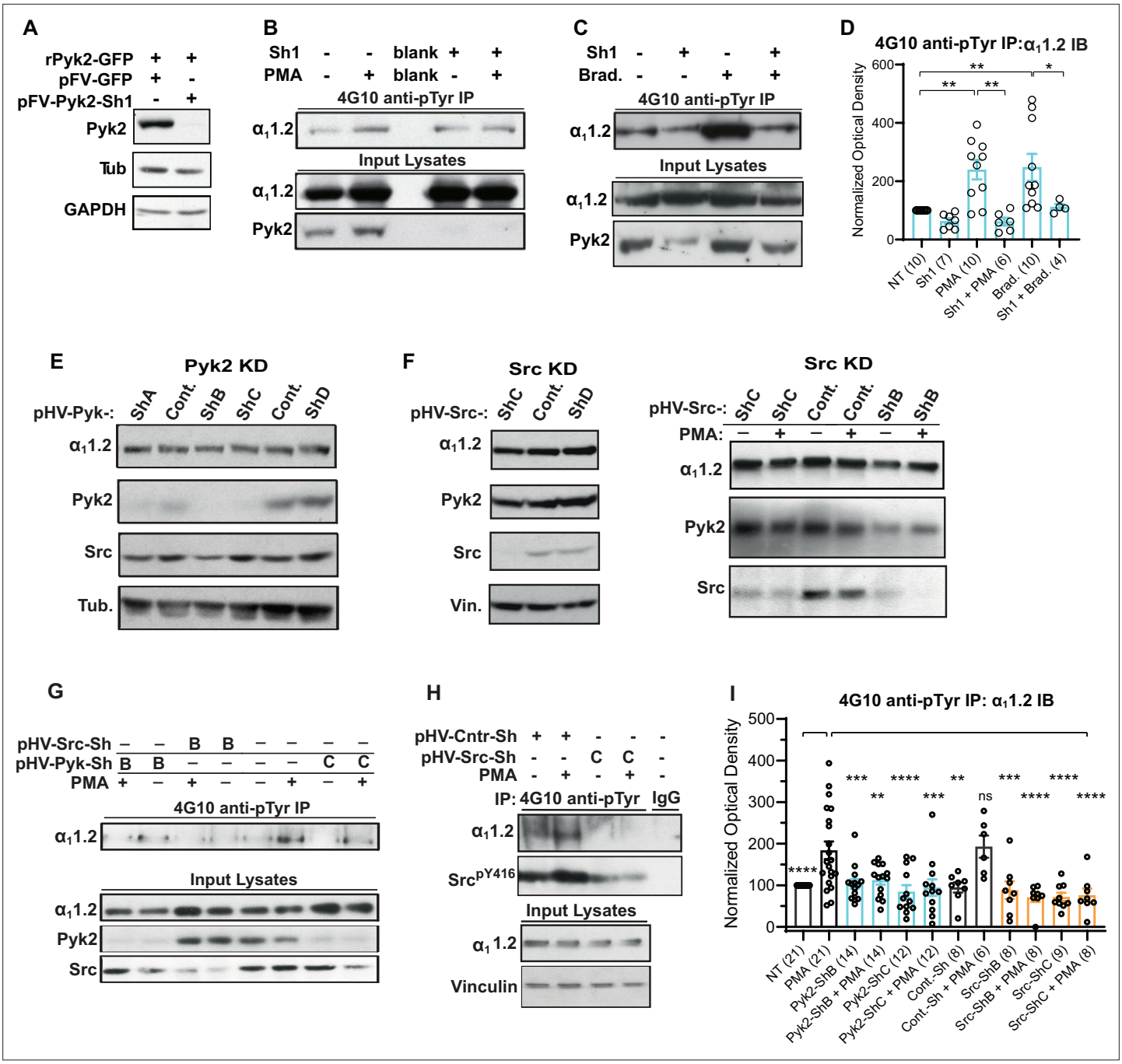

Figure 10. Increase in $\alpha_1$1.2 tyrosine phosphorylation by PKC is blocked by knockdown of Pyk2 and Src. (**A**) Lysates from HEK293T/17 cells transfected with vectors encoding rat Pyk2 (rPyk2-GFP) and either the Pyk2-targeting FIV lentivirus-derived, pVETL-Sh1-GFP (pFV-Pyk2-Sh1) or control (empty) pVETL-GFP (pFV-GFP) expression vectors, were immunoblotted (IB) with indicated antibodies. (**B, C**) IB analysis of indicated proteins in PC12 cultures incubated with viral particles containing pFV-Sh1-GFP (Sh1) FIV-based expression vector used in A or medium vehicle alone for 72 hr prior to treatment with either phorbol-12-myristate-13-acetate (PMA, **B**), bradykinin (Brad.; **C**), or vehicle alone (−; **B, C**). Upper blots in B and C show anti-$\alpha_1$1.2 IBs of 4G10-anti-phosphotyrosine (pY) immunoprecipitation (IP) while middle and lower blots show direct IBs of indicated protein levels in input lysates. (**D**) Statistical analysis of the relative pY $\alpha_1$1.2 levels. $F_{5,41}$ = 8.276. NT vs. PMA, p = 0.0031; NT vs. Brad., p = 0.0017; PMA vs. Sh1 + PMA, p = 0.001; Brad vs. Sh1 + Brad, p = 0.0433. (**E, F**) Direct IB analysis of indicated proteins in lysates of PC12 cultures transduced with HIV vector-derived lentiviral particles (e.g., pGFP-Pyk2-ShB-Lenti) containing expression cassettes for GFP and either the Pyk2-targeting (denoted pHV-Pyk-ShB and -ShC), Src-targeting (denoted pHV-Src-ShC and -ShD), or scrambled hairpin control (Cont.) shRNAs. In some cases (right blot in F) cultures were treated with PMA (+) or vehicle alone (−) before harvesting for IB. (**G, H**) IB analysis of indicated proteins from PC12 cultures infected with lentiviral particles containing HIV-GFP expression vectors as in E and F prior to treatment with either PMA (+) or vehicle (−). Upper panels show anti-$\alpha_1$1.2 IBs of 4G10-anti-pY IP while lower

Figure 10 continued on next page

Figure 10 continued

blots show direct IBs of input lysates with indicated antibodies. (**I**) Statistical analysis of relative $\alpha_1$1.2 pY levels. $F_{11,129}$ = 6.180. NT vs. PMA, p < 0.0001; PMA vs. Pyk2-ShB, p = 0.0005; PMA vs. Pyk2-ShB + PMA, p = 0.0029; PMA vs. Pyk2-ShC, p < 0.0001; PMA vs. Pyk2-ShC + PMA, p = 0.0002; PMA vs. Cont.-Sh, p = 0.0019; PMA vs. Cont.-Sh + PMA, p > 0.9999; PMA vs. Src-ShB, p = 0.0007; PMA vs. Src-ShB + PMA, p < 0.0001; PMA vs. Src-ShC, p < 0.0001; PMA vs. Src-ShC + PMA, p < 0.0001. The bar graphs in (D) and (I) show ratios of quantified anti-$\alpha_1$1.2 IB signals in 4G10 IPs relative to $\alpha_1$1.2 IB signals in total lysates, normalized to not treated (NT) control. Comparisons are made between samples treated with PMA (or bradykinin in D) and each of the other indicated conditions. Data are presented as mean ± standard error of the mean (SEM). Number (*n*) of independent experiments for each condition are indicated inside bars. Statistical analysis by analysis of variance (ANOVA) with post hoc Bonferroni's multiple comparisons test (ns = not significant vs. PMA, *p ≤ 0.05, **p ≤ 0.01, ***p ≤ 0.001, ****p ≤ 0.0001).

The online version of this article includes the following source data for figure 10:

Source data 1. Original files of the full raw unedited blots with bands labeled in red boxes.

glutamate receptors (mGluR) (***Wang et al., 2016***). We tested whether increasing Ca_V1.2 activity through α_1AR–PKC–Pyk2–Src signaling can augment LTP_{LTCC}. Similar to previous reports (***Boric et al., 2008***; ***Shankar et al., 1998***), LTP_{LTCC} was ~10% and was not statistically significant above baseline in our 13- to 20-week-old mice (***Figure 11A***). However, when Ca_V1.2 activity was upregulated by stimulation of α_1ARs with PHE, robust LTP_{LTCC} occurred (p ≤ 0.05, ***Figure 11A***). This augmentation of LTP_{LTCC} was completely blocked by the LTCC inhibitor nimodipine and the α_1AR antagonist prazosin (both p ≤ 0.001, ***Figure 11A***). Thus, this elevated potentiation strictly depends on both the activity of LTCCs and signaling through α_1ARs. Importantly, this LTP_{LTCC} is also blocked by the Pyk2 inhibitor PF-719 and the Src inhibitor PP2 (both p ≤ 0.001, ***Figure 11B***). These data indicate that robust LTP_{LTCC} in 13- to 20-week-old mice requires Pyk2 and Src activity downstream of engaging α_1AR to boost LTCC activation to sufficient levels.

Discussion

NE is arguably the most important neuromodulator for alertness and attention, augmenting multiple behavioral and cognitive functions (***Berman and Dudai, 2001***; ***Cahill et al., 1994***; ***Carter et al., 2010***; ***Hu et al., 2007***; ***Minzenberg et al., 2008***). The G_q-coupled α_1AR has a higher affinity for NE than βARs and has been implicated in many studies in attention and vigilance (***Bari and Robbins, 2013***; ***Berridge et al., 2012***; ***Hahn and Stolerman, 2005***; ***Hvoslef-Eide et al., 2015***; ***Liu et al., 2009***; ***Puumala et al., 1997***; ***Robbins, 2002***). Inspired by our earlier findings that Ca_V1.2 forms a unique signaling complex with β_2AR, G_s, AC, and PKA, making it a prominent effector of NE (***Davare et al., 2001***; ***Patriarchi et al., 2016***; ***Qian et al., 2017***), we tested and found that Ca_V1.2 is also a main target for NE signaling via the α_1AR. Given that Ca_V1.2 fulfills numerous functions in many cells this is a key and critical finding (***Jacquemet et al., 2016***; ***Splawski et al., 2004***). In the following paragraphs, we discuss the four central and notable outcomes of our study.

Firstly, we found that stimulation of the α_1AR or the BK receptor strongly increased LTCC activity in neurons (***Figures 1, 2, and 4–6***). Stimulation of two other major classes of G_q-coupled receptors in neurons, mGluR1/5 and muscarinic M1/3/5 receptors affected LTCC activity at the cell soma only modestly or not at all, respectively (***Figure 2—figure supplement 1***). Accordingly, G_q-mediated signaling augments LTCC activity upon stimulation of defined but not all G_q-coupled receptors. Thus, activity of LTCCs is selectively regulated by α_1AR and BK receptor signaling. Perhaps G_q-coupled mGluR and muscarinic receptors are not as close to the LTCCs that were recorded in somata than the α_1AR or BK receptor, limiting their contribution to regulating Ca_V1.2. Defining what restricts the receptor type that can regulate LTCCs will be an interesting avenue of future investigation.

Remarkably, inhibitors of PKC, Pyk2, and Src reduce under nearly all conditions Ca_V1.2 baseline activity and also tyrosine phosphorylation of Ca_V1.2, Pyk2, and Src even when activators for α_1AR and PKC were present. Especially notable is the strong reduction of channel activity way below the control conditions by the Src inhibitor PP2 as well as the PKC inhibitor chelerythrine in ***Figure 2C***. This effect is consistent with PP2 strongly reducing down below control conditions tyrosine phosphorylation of Src (***Figure 8J***), Pyk2 (***Figure 8L***), and Ca_V1.2 (***Figure 9E***) even with the PKC activator PMA present. These findings suggest that Pyk2 and Src experience significant although clearly by far not full activation under basal conditions as reflected by their own phosphorylation status, which translates into tyrosine phosphorylation of Ca_V1.2 under such basal conditions.

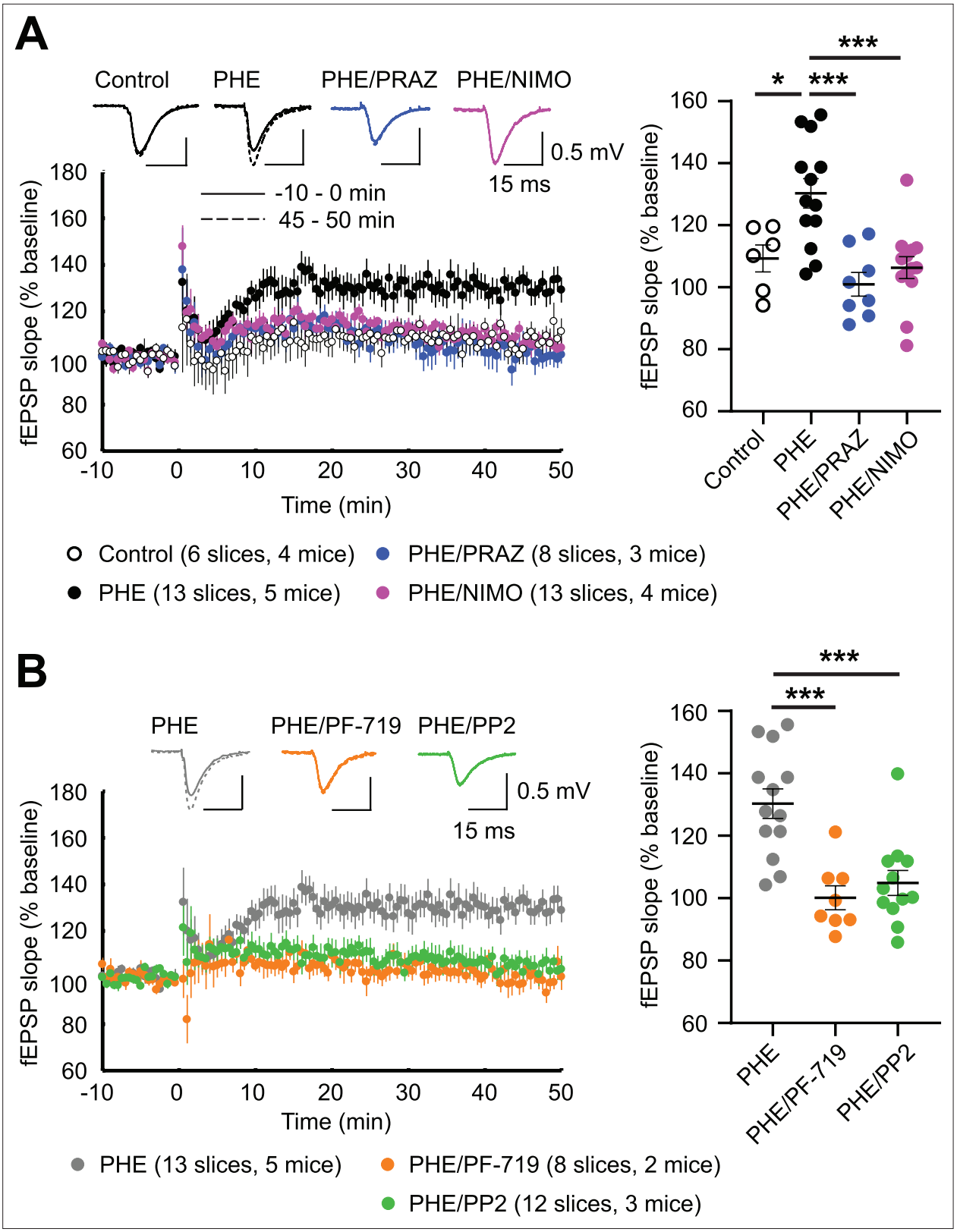

Figure 11. α_1AR signaling augments LTP_{LTCC} through L-type Ca^{2+} channel (LTCC) activity, Pyk2, and Src. LTP_{LTCC} was induced by four 200 Hz tetani, each 0.5 s long, in the CA3 Schaffer collateral projections to CA1 in acute hippocampal slices from 13- to 20-week-old mice. (**A**) LTP_{LTCC} required phenylephrine (PHE; 10 μM) and was prevented by the LTCC blocker nimodipine (10 μM; NIMO) and the α_1AR antagonist prazosin (1 μM; PRAZ). $F_{3,36}$ = 9.937. Control vs. PHE, p = 0.012; PHE vs. PHE/PRAZ, p = 0.0001; PHE vs. PHE/NIMO, p = 0.0003. (**B**) PHE-mediated long-term potentiation (LTP) is

Figure 11 continued on next page

Figure 11 continued

blocked by inhibitors of Pyk2 (1 μM PF-719) and Src (10 μM PP2). $F_{2,30}$ = 13.90. PHE vs. PHE/PF-719, p = 0.0002; PHE vs. PHE/PP2, p = 0.0003. Dot plots on the right show potentiation of field excitatory postsynaptic potentials (fEPSPs) determined as the averages of all responses between 45 and 50 min after high-frequency stimulation (HFS) as % of averages of all responses in the 5 min preceding HFS. Bars and whiskers represent means ± standard error of the mean (SEM; *p ≤ 0.05, ***p ≤ 0.001; one-way analysis of variance [ANOVA] with the Bonferroni correction). The number of slices and mice used is indicated.

Secondly, we identified a complex PKC/Pyk2/Src cascade that mediates regulation of $Ca_V1.2$ by the α_1AR. Clear evidence for this signaling pathway is provided by the inhibition of PHE-induced upregulation of LTCC activity by inhibitors of PKC, Pyk2, and Src (***Figure 2***), which is further supported by the finding that direct stimulation of PKC also upregulates LTCC activity via Pyk2 and Src (***Figure 3***). The role of the PKC/Pyk2/Src pathway in regulating $Ca_V1.2$ is also substantiated by the association of Pyk2 in addition to Src and PKC with $Ca_V1.2$ (***Figure 7***) and inhibition of PKC-induced tyrosine phosphorylation of $Ca_V1.2$ by Pyk2 and Src inhibitors (***Figure 9***) and Pyk2 and Src knockdown (***Figure 10***). Multiple shRNAs specifically targeting both Pyk2 and Src efficiently prevented the PKC-mediated increase in $\alpha_1$1.2 tyrosine phosphorylation. These observations not only confirm that Pyk2 mediates the $Ca_V1.2$ regulation downstream of PKC but also indicates that Src itself is in this context a relevant member of the Src kinase family.

Thirdly, we found that Pyk2 is firmly associated with $Ca_V1.2$ under basal conditions as reflected by their co-IP (***Figure 7***). This association places Pyk2 into a complex that also contains its immediate upstream activator and downstream effector, that is, PKC and Src. PKC can directly bind to the distal C-terminal region of $\alpha_1$1.2, which also contain S1928 (***Yang et al., 2005***). Given that S1928 is a phosphorylation site for PKC (***Yang et al., 2005***), it is conceivable that PKC binding to this region reflects a temporary kinase–substrate interaction rather than a more permanent association of PKC with $Ca_V1.2$, although this consideration does not rule out that PKC can stably bind to another region in the C-terminus of $\alpha_1$1.2. In addition, the A kinase anchor protein AKAP150, which is a major interaction partner for $Ca_V1.2$ (***Davare et al., 1999***; ***Hall et al., 2007***; ***Oliveria et al., 2007***), binds not only PKA but also PKC (***Klauck et al., 1996***) and constitutes another potentially constitutive link between PKC and $Ca_V1.2$ (***Navedo et al., 2008***). Furthermore, like Pyk2, Src co-precipitates with $Ca_V1.2$ (***Figure 7***) and binds directly to $\alpha_1$1.2 (***Bence-Hanulec et al., 2000***; ***Chao et al., 2011***; ***Hu et al., 1998***). Our determination that Pyk2 co-precipitates with $Ca_V1.2$ from not only brain but also heart indicates that $Ca_V1.2$ forms a signaling complex with Pyk2 and Src and possibly also PKC in various tissues.

We identified the loop between domains II and III of $\alpha_1$1.2 as the binding site for Pyk2. This observation lends further support to the association of Pyk2 with $Ca_V1.2$. Of note, Src binds to residues 1955–1973 in rat brain $\alpha_1$1.2 (corresponding to residues 1982–2000 in the original rabbit cardiac $\alpha_1$1.2 ***Mikami et al., 1989***; ***Bence-Hanulec et al., 2000***; ***Chao et al., 2011***). This interaction with $\alpha_1$1.2 might bring Src in close proximity to loop II/III-associated Pyk2 to augment their structural and functional interaction once Pyk2 has been activated by PKC.

Formation of supramolecular signaling complexes or 'signalosomes' consisting of kinases and their 'customers' ensures fast, efficient, and specific signaling (***Dai et al., 2009***; ***Dodge-Kafka et al., 2006***). Our work establishes the PKC–Pyk2–Src–$Ca_V1.2$ complex as such a signalosome. Furthermore, it defines how various G_q-coupled receptors stimulate the activity of $Ca_V1.2$ in different cells. The remarkably strong upregulation of $Ca_V1.2$ channel activity by Src (***Bence-Hanulec et al., 2000***; ***Gui et al., 2006***) and upon activation of the PKC–Pyk2–Src signaling cascade as shown here rivals the upregulation by β-adrenergic signaling, which is a central and thus widely studied mechanism of regulating Ca^{2+} influx into cardiomyocytes during the fight or flight response (***Balijepalli et al., 2006***; ***Bean et al., 1984***; ***Fu et al., 2013***; ***Fu et al., 2014***; ***Fuller et al., 2010***; ***Lemke et al., 2008***; ***Liu et al., 2020***; ***Reuter, 1983***). Of note, $Ca_V1.2$ assembles all components required for β-adrenergic signaling including the β_2AR, G_s, adenylyl cyclase, and PKA in brain (***Davare et al., 2001***; ***Davare et al., 1999***; ***Man et al., 2020***) and heart (***Balijepalli et al., 2006***). Formation of this complex is important for upregulation of $Ca_V1.2$ activity (***Balijepalli et al., 2006***; ***Patriarchi et al., 2016***) and LTP of glutamatergic synapses induced by a 5-Hz theta rhythm during β-adrenergic stimulation (***Patriarchi et al., 2016***; ***Qian et al., 2017***). Analogously, assembly of the PKC–Pyk2–Src–$Ca_V1.2$ signalosome may be important for fast and specific regulation of $Ca_V1.2$ by the α_1AR. This hypothesis can now be tested by pursuing determination of the precise binding site of Pyk2 in the loop between domains II and III

of $\alpha_1$1.2 and then disrupting this interaction with peptides and point mutations. However, our initial attempts to narrow down the binding region by binding studies with six synthetic ~25 residue long overlapping peptides that spanned loop II/III failed (data not shown). Perhaps the Pyk2-binding site in loop II/III requires tertiary structural elements or sequences that were distributed between two neighboring peptides (which overlapped by five residues).

In rat brain neurons, LTCC activity can be increased by Src via phosphorylation of $\alpha_1$1.2 on Y2122 (***Bence-Hanulec et al., 2000***; ***Gui et al., 2006***). However, this phosphorylation site is not conserved even within rodents. It is equivalent to position 2150 in rabbit cardiac $\alpha_1$1.2, which is a Cys and not Tyr residue (***Mikami et al., 1989***). Accordingly, other Tyr residues must serve as phosphorylation sites. It will be an interesting challenge for future work to identify the exact phosphorylation site and then test its functional relevance.

Remarkably, the Src inhibitor PP2 also completely blocked PKC-induced autophosphorylation of Pyk2 on Y402 (***Figure 8K, L***). This finding indicates a close interdependence between Pyk2 and Src activation by PKC in PC12 cells (depicted in ***Figure 8A***). It is consistent with earlier results indicating that Pyk2 activation (assessed by Y402 phosphorylation) requires catalytically active Src (***Cheng et al., 2002***; ***Shi and Kehrl, 2004***; ***Sorokin et al., 2001***; ***Zhao et al., 2016***), although in other systems Y402 phosphorylation was not dependent on Src (***Corvol et al., 2005***; ***Park et al., 2004***; ***Yang et al., 2013***). Accordingly, Pyk2 autophosphorylation on Y402 and the consequent binding of Src to phosphoY402 induces Src-mediated phosphorylation of Pyk2 on Y579 or Y580 in its activation loop, which further enhances Pyk2 activity beyond the level achieved by Pyk2 autophosphorylation on Y402 (***Dikic et al., 1996***; ***Lakkakorpi et al., 2003***; ***Li et al., 1999***; ***Park et al., 2004***). Such interdependence was supported by the observation that Y579 phosphorylation upon PKC stimulation by either PMA or BK was also completely blocked by the Src inhibitor PP2 (***Figure 8K, M***).

Fourthly and finally, LTP_{LTCC} induced by 200 Hz tetani in 13- to 20-week-old mice required stimulation of α_1ARs and is completely blocked by inhibitors of LTCC, Pyk2, and Src (***Figure 11***). Incidentally, we were not able to induce any LTP_{LTCC} in mice younger than 13 weeks. Taken together, our findings suggest that LTP_{LTCC} requires stimulation of Ca_V1.2 activity by α_1AR–PKC–Pyk2–Src signaling. While we focus here on the importance of α_1AR signaling for LTP_{LTCC}, this is not the only form of LTP that requires upregulation of Ca^{2+} influx through Ca_V1.2. Prolonged theta tetanus LTP (PTT-LTP), which is induced by a 3-min-long 5 Hz tetanus, also depends on upregulation of Ca_V1.2 activity (***Boric et al., 2008***; ***Cavuş and Teyler, 1996***; ***Grover and Teyler, 1990***; ***Moosmang et al., 2005***; ***Wang et al., 2016***). In PTT-LTP, this upregulation is accomplished by β_2AR–G_s–adenylyl cyclase/cAMP–PKA signaling and the ensuing phosphorylation of the central pore-forming $\alpha_1$1.2 subunit of Ca_V1.2 on S1928 by PKA (***Patriarchi et al., 2016***; ***Qian et al., 2012***; ***Qian et al., 2017***). Whether signaling by NE through α_1AR and β_2AR can act in parallel and is additive will be an interesting question for future studies. However, we already know that at least for classic PTT-LTP β_2AR signaling is sufficient and does not require engagement of α_1AR signaling (***Qian et al., 2012***). Because regulation of Ca_V1.2 by β_2AR signaling is highly localized (***Davare et al., 2001***; ***Patriarchi et al., 2016***), it is conceivable that α_1AR signaling might engage a subpopulation of Ca_V1.2 channels whose spatial distribution differs from that of β_2AR-stimulated Ca_V1.2 in dendrites. Alternatively, parallel engagement of α_1AR and β_2AR signaling might ensure more robust and possibly additive or synergistic responses both at the Ca_V1.2 channel level and in the synaptic potentiation that results.

LTP is thought to underlie learning and memory (***Choi et al., 2018***; ***Whitlock et al., 2006***). Conditional knock out of Ca_V1.2 in the hippocampus and forebrain impaired LTP_{LTCC} as well as initial learning (***Moosmang et al., 2005***) and long-term memory of spatial Morris water maze tasks (***White et al., 2008***). Moreover, decreased Ca_V1.2 expression or infusion of LTCC blockers into the hippocampus impaired both, LTP induced by pairing backpropagating action potentials in dendrites with synaptic stimulation and latent inhibition (LI) of contextual fear conditioning, the latter requiring learning to ignore non-relevant environmental stimuli (***Tigaret et al., 2021***). These Ca_V1.2-related learning deficits might be in part due to impaired attention the animals pay to their experimental environment during learning phases, processes requiring concerted attention (***Panichello and Buschman, 2021***). Attention, in turn, depends on the neurotransmitter NE, which might augment spatial learning through regulation of Ca_V1.2 via α_1AR–PKC–Pyk2–Src signaling.

Ca_V1.2 is increasingly implicated in not just the postsynaptic physiological functions discussed above. Multiple genome-wide association studies point to variants in the Ca_V1.2 gene, *CACNA1C*,

as major risk factors for schizophrenia, bipolar disorder, and other mental diseases (***Bhat et al., 2012***; ***Ferreira et al., 2008***; ***Green et al., 2010***; ***Nyegaard et al., 2010***; ***Smoller, 2013***; ***Splawski et al., 2004***). Other studies link chronic upregulation of $Ca_V1.2$ activity to etiologies behind senility and Alzheimer's disease (e.g., ***Davare and Hell, 2003***; ***Deyo et al., 1989***; ***Disterhoft et al., 1994***; ***Thibault and Landfield, 1996***). Thus, it appears likely that dysfunctional regulation of $Ca_V1.2$ contributes to these diseases, making the detailed molecular analyses of the signaling paradigms that regulate its functionality especially important to advance our mechanistic understanding for development of future therapies.

Here, we establish for the first time that NE upregulates $Ca_V1.2$ activity via a complex α_1AR signaling cascade through PKC, Pyk2, and Src, the activity of each component being essential for LTP_{LTCC} and thus most likely relevant for learning. Our work forms the foundation for future studies to uncover the physiological context in which this action of NE is specifically engaged, what the precise role for each kinase is in this signaling cascade regulating $Ca_V1.2$ activity, and how the individual kinases could be coordinately regulated to further fine-tune $Ca_V1.2$ function. Given the central role of NE in attention and the many physiological and pathological aspects of $Ca_V1.2$, regulation of this channel via NE–α_1AR signaling predictably will elicit widespread and profound functional effects.

Materials and methods

Materials availability statement

Further information and requests for resources and reagents should be directed to and will be fulfilled by the corresponding authors, Mary C. Horne (mhorne@ucdavis.edu) and Johannes W. Hell (jwhell@ucdavis.edu).

Experimental model and subject details

Animals

Pregnant Sprague-Dawley (SD) rats were ordered from Envigo (Order code 002) or Charles River (Strain code 001) and E18 embryos were used for preparation of dissociated hippocampal neuronal cultures. SD rats used for preparation of tissue extracts from heart and brain were of either sex and around 3 months old. For LTP experiments, mice of the strain B6129SF1/J aged between 13 and 18 weeks (both males and females) were used.

Animals were maintained with a 12/12 hr light/dark cycle and were allowed to access food and water ad libitum. All procedures followed NIH guidelines and had been approved by the Institutional Animal Care and Use Committee (IACUC) at UC Davis (Protocol # 20673 and 22403).

Primary hippocampal neuronal cultures

Primary hippocampal neurons were maintained at 37°C in humidified incubators under 5% CO_2 and 95% air. Both male and female rat embryos were used to prepare the cultures. Neurons were maintained in a medium containing 1× B-27 supplement (Gibco Cat#17504044), 1× Glutamax (Gibco Cat#35050061), 5% fetal bovine serum (FBS, Corning Cat#35-010-CV), and 1 µg/ml gentamicin (Gibco Cat#15710-064) in Neurobasal medium (Gibco Cat#21103-049). 10 µM each of 5-fluoro-2′-deoxyuridine (Sigma-Aldrich Cat#F0503) and uridine (Sigma-Aldrich Cat#U3003) were added around DIV7 to block the growth of glial cells.

Cell lines

All cells were grown at 37°C in humidified incubators under 5% CO_2 and 95% air. Rat pheochromocytoma cell line PC12 (ATCC Cat# CRL-1721; RRID:CVCL_0481, male) was grown in RPMI 1640 media (Gibco Cat#11875-101) containing 10% horse serum (HS, Gemini Bio Products Cat#100-508) and 5% FBS. For serum starvation, PC12 were incubated for 18 hr in RPMI 1640 media containing 1% HS and 0.5% FBS. HT-1080 cells (ATCC CCL-121; RRID:CVCL_0317, male) used for virus titration were grown and maintained in MEM (Gibco Cat#11095-080) supplemented with 10% FBS. HEK293T/17 (ATCC Cat# CRL-11268, RRID:CVCL_1926, female) cells were routinely cultured in Dulbecco's Modified Eagle Medium (DMEM) supplemented with 10% FBS (Gibco Cat#11995-065). Cell lines used were obtained from ATCC, expanded and frozen at low passage number. Care was taken during the use of cell lines to ensure that only one cell line was processed in the culture hood at a time, and that

they were used within 25–30 passages. Their morphology in culture and doubling time were routinely monitored as were other distinguishing properties such as high transfectability (HEK293T/17 cells) or high $Ca_V1.2$ expression (PC12 cells) before the time of experimental use.

Authentication of cell lines

All three cell lines HEK293T/17, HT1080,and PC12 cells were obtained from ATCC, a well-established and highly reliable source for cell lines. These are the only cell lines currently used in our lab, minimizing further any potential for confusion.

HEK293T/17 was only used for production of virus for knockdown of Pyk2 and Src and initial testing for efficacy of respective knockdown and not for data collection. It was mostly authenticated by inspection of shape and determination of viability as well as the absence of voltage-gated ion channels including $Ca_V1.2$ as tested electrophysiologically (all hallmarks of endothelial cells like HEK293 cells). All viruses produced with this cell line were of the expected titer and infectivity as tested. Further, the knockdown results for ectopically expressed Pyk2 and Src in these HEK293T cells were consistent with subsequent knockdown of endogenous Pyk2 and Src in our PC12 cells by several viruses with respective shRNA (***Figure 9*** and data not shown).

HT1080 was exclusively used for testing viral titer and mostly authenticated by inspection of shape and determination of viability.

PC12 cells are derived from a pheochromocytoma tumor and were verified in different ways. Firstly, they had the typical appearance described earlier, with some 'rugged' edges under basal conditions. Upon addition of nerve growth factor (NGF) they adopted a more neuron-like appearance with elongated protrusions reminiscent of short neurites. This response to NGF is a clear hallmark of PC12 cells and the reason why they are popular for use in biochemical experiments when neuron-like cultured cells are needed. Additional parameters were expression of L-type Ca channels as determined electrophysiologically (data not shown) and biochemically specifically for $Ca_V1.2$ as thoroughly analyzed in this study (***Figures 8–10***). In addition, expression of the BK receptor and its downstream effectors Pyk2 and Src is known to be very prominent in PC12 cells. (Pyk2 was first identified in PC12 cells) and again regularly observed in our thorough biochemical analysis.

Test for mycoplasma was performed per commercial PCR and was negative.

Methods details

Culture of primary hippocampal neurons

Hippocampal neurons were cultured from wild-type E18 male and female embryos from SD rats. Hippocampus was excised from the brains of embryos in ice-cold Hank's Buffer (Sigma-Aldrich Cat#H2387) with 10 mM 4-(2-Hydroxyethyl)-1-piperazineethanesulfonic acid (HEPES) (Gibco Cat#15630-080), 0.35 g/l $NaHCO_3$ and 5 µg/ml gentamicin (Gibco Cat#15710-064) and digested in 0.78 mg/ml papain (Roche Cat#10108014001) in 5 ml of the same buffer at 37°C for 30 min, in an incubator containing 5% CO_2 and 95% air. Digested hippocampal tissue was washed with neuron medium twice, and triturated in the medium. The medium used for washes, trituration and culture of neurons consists of 1× B-27 supplement, 1× Glutamax, 5% FBS, and 1 µg/ml gentamicin in Neurobasal medium (as stated in Experimental model and subject details). 15,000 neurons were plated per well in 24-well plates on coverslips coated with poly-DL-ornithine (Sigma-Aldrich Cat#P0671) and laminin (Corning Cat#354232) and cultured in an incubator at 37°C and 5% CO_2 and 95% air.

Single-channel recording – determination of overall channel activity (N × Po)

Single-channel recording was performed at room temperature on hippocampal neurons on DIV10–15 using the cell-attached configuration at an Olympus IX50 inverted microscope as before (***Patriarchi et al., 2016***; ***Qian et al., 2017***). The membrane potential was fixed at ~0 mV using a high K^+ external solution. The external (bath) solution contained (in mM) 145 KCl, 10 NaCl, 10 HEPES, and 30 D-glucose (pH 7.4 with NaOH, 325–330 mOsM). The internal (pipette) solution contained 110 mM $BaCl_2$, 20 mM tetraethylammonium chloride (TEA-Cl), 10 mM HEPES, 500 nM BayK 8644 (Tocris Cat#1546; 200 nM used for ***Figures 1 and 2***; 500 nM used for ***Figure 3***), and 1 µM each of ω-conotoxins MVIIC and GVIA (China Peptides, custom synthesized) (pH 7.2 with TEA-OH, 325–330 mOsM). 3.5–5.5 MΩ resistance pipettes were used. The concentrations of kinase inhibitors, α_1AR receptor blocker and agonist are as indicated in the figure legends. Neurons were preincubated

with kinase inhibitors or receptor blocker in culture medium for 10 min prior to the experiment, and kinase inhibitors and receptor blocker were, where relevant, present in the external solution during recording. In experiments where isradipine was used, it was placed in the pipette solution, and no pre-incubation with isradipine was performed. Recordings started within 10 min of placing coverslips in the recording chamber in a bath solution with or without PHE (Sigma-Aldrich Cat#P6126), PMA (Merck Millipore Cat#524400), and different kinase inhibitors and receptor blocker. Currents were sampled at 100 kHz and low-pass filtered at 2 kHz using an Axopatch 200B amplifier (Axon Instruments) and digitized using Digidata 1440A digitizer (Axon Instruments). Step depolarizations of 2-s duration (one sweep) were elicited to the patch from −80 to 0 mV at a start-to-start stimulation interval of 7 s. Typically, 100 sweeps were recorded per neuron and only cells with more than 70 sweeps recorded were analyzed. The single-channel search event detection algorithm of Clampfit 10.7.0.3 (Axon Instruments) was used to analyze single-channel activities. Ensemble average traces were computed by averaging all sweeps from one neuron and averaging the averaged traces from all neurons in each group.

Single-channel recording – determination of Po

To specifically determine unitary channel open probability Po, borosilicate pipettes with a resistance of 7–12 MΩ were used. Only patches with no more than 4 channels ($k \leq 4$) were included in the Po analysis to not overinterpret Po (***Horn, 1991***). Data were corrected by the number of channels ($k = 1$) as previously described (***Bartels et al., 2018***; ***Turner et al., 2020***). Unitary LTCC events from hippocampal neurons (DIV15–25) where isolated through blocking N/P/Q-type calcium channels by using 1 µM each of ω-conotoxins MVIIC and GVIA (China Peptides, custom synthesized) in the patch pipette and recorded as above at room temperature by step depolarizations from −80 to 0 mV. Extracellular bath solution contained 125 mM K-glutamate, 25 mM KCl, 2 mM $MgCl_2$, 1 mM $CaCl_2$, 1 mM ethylene glycol bis(2-aminoethyl)tetraacetic acid (EGTA), 10 mM HEPES, 10 mM glucose, and 1 mM Na-ATP, pH 7.4 with KOH. Depolarizing pipette solution contained 110 mM $BaCl_2$ and 10 mM HEPES, adjusted to a pH of 7.4 with TEA-OH. Data acquisition was performed at a sampling frequency of 10 kHz with an interpulse time of 5 s and data were low pass filtered at 2 kHz. The positive identification of LTCC activity was consequently tested by bolus application of either the dihydropyridine (DHP) BayK8644 (10 µM), which promotes L-type channel opening, or the channel-blocking DHPs isradipine (10 µM) or nimodipine (10 µM) to the bath solution at the end of each experimental run.

Drugs

were prepared as stock solution in dH_2O, freshly on the day of experiment respectively, 40 mM prazosin–HCl (Sigma-Aldrich), 20 mM NE bitartrate (Sigma-Aldrich) and 20 mM BK acetate (Sigma-Aldrich). Stocks were diluted again 1:10 or 1:100 and as a bolus directly applied to the bath solution during the recordings.

Co-immunoprecipitation of $Ca_V1.2$ with Pyk2 and Src

Brains and hearts were homogenized with a Potter tissue homogenizer in 10 ml of a homogenization buffer containing 50 mM Tris–HCl (pH 7.4), 150 mM NaCl, 5 mM EGTA pH 7.4, 10 mM ethylenediaminetetraacetic acid (EDTA), 1% Triton X-100, 25 mM NaF, 25 mM sodium pyrophosphate, 1 mM 4-nitrophenyl phosphate, 2 µM microcystin and protease inhibitors (1 µg/ml leupeptin [Millipore Cat#108975], 2 µg/ml aprotinin [Millipore Cat#616370], 10 µg/ml pepstatin A [Millipore Cat#516481] and 200 nM phenylmethylsulfonyl fluoride [PMSF]). High-speed centrifugation was performed at 40,000 rpm for 30 min at 4°C. 500 µg of total brain or heart lysate extracts were incubated with 15 µl of Protein-A Sepharose beads (CaptivA protein resin, Repligen, Cat#CA-PRI-0100) and 2 µg of anti-$Ca_V1.2$ α1-subunit or control rabbit IgG antibody. Samples were incubated at 4°C for 4 hr before being washed three times with ice-cold wash buffer (0.1% Triton X-100 in 150 mM NaCl, 10 mM EDTA, 10 mM EGTA, 10 mM Tris, pH 7.4). Samples were then resolved by SDS–PAGE and transferred onto polyvinylidene difluoride (PVDF) membranes before IB with anti-$Ca_V1.2$ α1-subunit (J.W. Hell lab), -Pyk2 (Millipore Cat#05-488; RRID:AB_2174219), and -Src (J.S. Brugge lab) antibodies. The antibody dilutions used are listed in ***Supplementary file 2***.

GST pulldown assay

Fragments of intracellular loops of $Ca_V1.2$ α_1-subunit (***Supplementary file 1***; ***Davare et al., 2000***; ***Gao et al., 2001***) were expressed in *Escherichia coli* strain BL21 as GST fusion proteins, purified, and integrity verified by IB essentially as previously described (***Bennin et al., 2002***; ***Frangioni and Neel, 1993***; ***Hall et al., 2013***; ***Hall et al., 2006***). Overnight cultures from single colonies of the corresponding plasmids were cultured initially in 50 ml of LB medium containing ampicillin (100 µg/ml) with aeration until saturation. Incubation temperature was optimized for each expression construct to optimize translation and stability and varied between 28 and 37°C. After a 1:10 dilution into the same medium, cultures were grown for about 2–4 hr until an A600 of about 0.8 was reached when isopropyl-β-D-thiogalactopyranoside was added for induction. After 4–5 hr bacteria were collected by centrifugation (5000 rpm, SLA 3000 rotor, Thermo Fisher Cat#07149) for 15 min and resuspended by gentle trituration in ice-cold 50 ml of Tris-buffered saline (TBS) Buffer (150 mM NaCl, 15 mM Tris-Cl, pH 7.4) containing protease inhibitors 1 µg/ml pepstatin A, 1 µg/ml leupeptin, 1 µg/ml aprotinin, and 200 nM PMSF. 0.1 mg/ml lysozyme was added to lyse cell walls. The mixture was kept on ice for 30 min before addition of Sarcosyl (1.5% final concentration), β-mercaptoethanol (10 mM), and DNAse (50 U) for 15 min to fully solubilize the fusion proteins. In order to neutralize Sarcosyl, Triton X-100 was then added to a final concentration of 5%. Insoluble material was removed by ultracentrifugation (1 hr, 4°C, 40,000 rpm, Ti70 rotor, Beckman Coulter Cat#337922). The fragments were immobilized onto glutathione Sepharose (Millipore/Cytiva Cat#17-5132-02) for 3 hr, washed three times with Buffer A (0.1% TX-100, 10 mM Tris–HCl, pH. 7.4) and incubated with affinity-purified His-tagged Pyk2 separately expressed in *E. coli* (3 hr, 4°C). Beads were washed three times in Buffer A and bound proteins were eluted and denatured in SDS sample buffer, resolved by SDS–PAGE and transferred to a nitrocellulose membrane. IB with anti-Pyk2 antibody (Millipore Cat#05-488; RRID:AB_2174219) was used to detect Pyk2 binding during pulldown.

Analysis of phosphorylation in PC12 cells

Drugs were used at the following concentrations: 2 µM PMA (Merck Millipore Cat#524400), 1 µM BK (Sigma-Aldrich Cat#05-23-0500), 3 µM PF-431396 (Tocris Cat#4278), 10 µM PP2 (Sigma-Aldrich Cat#P0042), 10 µM PP3 (Tocris Cat#2794), and 10 µM SU6656 (Sigma-Aldrich Cat#S9692).

For phospho-tyrosine analysis PC12 cells were washed after drug treatment twice in ice-cold phosphate-buffered saline (PBS) containing 1 mM pervanadate and 25 mM NaF. Samples were collected in PBS containing pervanadate, NaF, and protease inhibitors (see above), sonicated and extracted with SDS dissociation buffer (50 mM Tris–HCl, 1% SDS) at 65°C for 10 min. The SDS was neutralized with a fivefold excess of Buffer A containing phosphatase and protease inhibitors. 500 µg of total protein from PC12 cell extracts were incubated over night at 4°C with 2 µg of the phospho-tyrosine 4G10 (Sigma-Alrich/Upstate Cat# 05-321; RRID:AB_2891016) or mouse control antibody (Jackson Immunoresearch Cat#015-000-003) and 15 µl of Protein-G Sepharose (Millipore/Cytiva Cat#GE-17-0618-05), washed three times in ice-cold wash buffer (0.1% Triton X-100 in 150 mM NaCl, 10 mM EDTA, 10 mM EGTA, 10 mM Tris, pH 7.4), resolved by SDS–PAGE and transferred onto PVDF membranes for IB. The antibody dilutions used are listed in ***Supplementary file 2***. For re-probing, blots were stripped in 62.5 mM Tris-Cl, 20 mM dithiothreitol (DTT), and 2% SDS at 50°C for 30 min. Chemiluminescence immunosignals were quantified using ImageJ (***Rueden et al., 2017***) by multiple film exposures of increasing length to ensure signals were in the linear range (***Davare and Hell, 2003***; ***Hall et al., 2006***). Variations in total amounts of $\alpha_1$1.2, Pyk2, and Src in the different PC12 cell lysates were monitored by direct IB of lysate aliquots. Lysate signals were used to correct $\alpha_1$1.2 signals after 4G10 IP for such variations by dividing the latter by the former.

Lentiviral constructs for shRNA to Pyk2 and Src

A list of all shRNA target sequences is provided in ***Supplementary file 3***. The shRNA sequence Sh1 against Pyk2 has been validated for Pyk2 knockdown (***Sayas et al., 2006***). The Sh1 sequence was cloned in the reverse orientation into the MfeI site of the lentiviral transfer vector pVETL-eGFP (***Bartos et al., 2010***; ***Boudreau and Davidson, 2012***; ***Harper et al., 2006***) for expression of Pyk2 shRNA and GFP to visualize infection. All HIV plasmids (HIV-GFP-Pyk2shA-D; HIV-GFP-SrcshA-D) for knocking down rat Pyk2 or Src as well as the scrambled, non-silencing hairpin control (HIV-GFP-shscr) were

obtained from Origene (Cat# TL710108 and #TL711639). All expression plasmids (listed in ***Supplementary file 4***) were confirmed by DNA sequencing.

Production of lentivirus for Pyk2 and Src knockdown

HEK293T/17 (ATCC Cat# CRL-11268, RRID:CVCL_1926) cells were plated onto 10 cm dishes at 1.8 × 10^6 cells per dish and maintained until confluency (60–90%). Cells were transiently transfected with viral expression constructs using the calcium phosphate precipitation method (***Jordan et al., 1996***). For FIV virus production, cells were transfected in a 3:2:1 ratio of parental vector (pVETL, FIV 3.2): pCPRD-Env: pCI-VSVG for a total of 24 µg of DNA per plate. For production of HIV viral particles targeting Src and Pyk2, cells were transfected at a ratio of 5:2:2:2 of parental vector (e.g., pGFP-Pyk2-shC-Lenti:pCI-VSVG:pMDL g/p RRE:pRSV-REV) according to the manufacturer's guidelines (OriGene). Media was exchanged 16 hr after transfection. Media containing the packaged recombinant virus was collected at 48 and 72 hr, filtered through 0.45 µm filters, and concentrated by centrifugation (7400 × *g* for 16 hr at 4°C). The viral pellet was resuspended in ice-cold PBS, aliquoted and stored at −80 °C. Before use for transduction of PC12 cells all viral particle solutions were titered in the HT-1080 cell line (ATCC Cat#CCL-121; RRID:CVCL 0317) by seeding 12-well plates at 5 × 10^4 cells per well 1 day before infection. 1, 5, and 10 µl of solutions containing concentrated HIV or FIV particles was added to each well and expression of GFP was monitored for 72 hr post-infection before titer was calculated.

Slice preparation and electrophysiology

After decapitation, brains were removed from 13- to 18-week-old mice. 400-µm-thick transverse slices were made using a vibratome in cold, oxygenated (95% O_2 and 5% CO_2) dissection buffer (in mM: 87 NaCl, 2.5 KCl, 1.25 NaH_2PO_4, 26.2 $NaHCO_3$, 25 glucose, 0.5 $CaCl_2$, 7 $MgCl_2$, 50 sucrose). Slices were allowed to recover at room temperature for at least 1 hr in oxygenated artificial cerebrospinal fluid (ACSF) (in mM: 119 NaCl, 3 KCl, 2.5 $CaCl_2$, 1.25 NaH_2PO_4, 1.3 $MgSO_4$, 26 $NaHCO_3$, 11 glucose). Following recovery, slices were transferred to a recording chamber and maintained at 32–33°C in oxygenated ACSF. Field excitatory postsynaptic potential (fEPSP) was evoked by stimulating the Schaffer collateral pathway using bipolar electrode, and synaptic responses were recorded with ACSF-filled microelectrodes (1–10 MΩ) placed in the stratum radiatum of CA1 region. Recordings were acquired using an Axoclamp-2B amplifier (Axon Instruments) and a Digidata 1332 A digitizer (Axon Instruments). Baseline responses were collected at 0.07 Hz with a stimulation intensity that yielded 40–50% of maximal response. LTP was induced by four episodes of 200 Hz stimulation (0.5 s) with 5-s intervals. To measure LTCC-mediated LTP, 50 µM D-APV (Tocris Cat#0106) was included in ACSF. When used the inhibitors [10 µM nimodipine (Bayer Charge: BXR4H3P), 1 µM prazosin, 1 µM PF-719 (***Tse et al., 2012***), and 10 µM PP2] were added to ACSF from the start of the recording. PHE (10 µM) was added after at least 15 min of stable baseline, and LTP was induced ~10 min after the addition of PHE.

Quantification and statistical analysis

Statistical analyses were performed using Prism 5 or 9 (GraphPad). Data are presented as mean ± standard error of the mean. Sample sizes, p values, and statistical tests are indicated in the figure legends. For analysis of channel NPo (***Figures 1–3***, ***Figure 2—figure supplement 1***, ***Figure 3—figure supplement 1***), first outliers were identified using iterative Grubb's method inbuilt in Prism. Then, statistical significance was determined using one-way analysis of variance (ANOVA) with post hoc Holm–Sidak's multiple comparisons test. For analysis of specifically Po (***Figures 4–6***), data were tested either by an unpaired or paired Student's *t*-test. For significance testing with more than two groups, a one-way ANOVA with additional Bonferroni correction was applied, $p < 0.05\%$. For analysis of protein phosphorylation, statistical significance was determined using ANOVA with post hoc Bonferroni's multiple comparisons test (***Figures 8–10***). For analysis of LTP (***Figure 11***), a one-way ANOVA was applied followed by Bonferroni correction.

Acknowledgements

We thank Dr. Stephen Strittmatter (Yale University) for providing PF-719. Dr. K Man executed the electrophysiological recordings shown in ***Figures 1–3***; Dr. P Bartels executed the electrophysiological

recordings shown in ***Figures 4–6***; Drs. Mei Shi and Mingxu Zhang performed the biochemical analysis in ***Figure 7***; Dr. Peter Henderson performed the biochemical analysis in ***Figures 8–10***; Dr. Karam Kim performed the LTP measurements in ***Figure 11***. FUNDING This work was supported by National Institutes of Health grant R01 NS123050 (JWH), National Institutes of Health grant RF1 AG055357 (JWH), National Institutes of Health grant R01 MH097887 (JWH), National Institutes of Health grant R01 HL098200 (MFN), National Institutes of Health grant R01 HL121059 (MFN), and National Institutes of Health grant T32 GM099608 (PBH).

Additional information

Funding

Funder	Grant reference number	Author
National Institutes of Health	R01 MH097887	Johannes W Hell
National Institutes of Health	RF1 AG055357	Johannes W Hell
National Institutes of Health	R01 HL098200	Manuel F Navedo
National Institutes of Health	R01 HL121059	Manuel F Navedo
National Institutes of Health	T32 GM099608	Peter B Henderson
National Institutes of Health	R01 NS123050	Madeline Nieves-Cintron

The funders had no role in study design, data collection, and interpretation, or the decision to submit the work for publication.

Author contributions

Kwun Nok Mimi Man, Conceptualization, Data curation, Formal analysis, Validation, Investigation, Visualization, Methodology, Writing - original draft, Project administration, Writing – review and editing; Peter Bartels, Data curation, Formal analysis, Validation, Visualization, Methodology, Writing – review and editing; Peter B Henderson, Resources, Data curation, Formal analysis, Funding acquisition, Validation, Investigation, Methodology; Karam Kim, Data curation, Formal analysis, Validation, Visualization, Methodology; Mei Shi, Data curation, Formal analysis, Validation, Investigation, Methodology; Mingxu Zhang, Data curation, Formal analysis, Investigation, Methodology; Sheng-Yang Ho, Data curation, Methodology; Madeline Nieves-Cintron, Data curation, Methodology, Writing – review and editing; Manuel F Navedo, Data curation, Funding acquisition, Methodology, Writing – review and editing; Mary C Horne, Conceptualization, Resources, Data curation, Formal analysis, Supervision, Validation, Investigation, Visualization, Methodology, Writing - original draft, Project administration, Writing – review and editing; Johannes W Hell, Conceptualization, Formal analysis, Supervision, Funding acquisition, Validation, Investigation, Visualization, Methodology, Writing - original draft, Project administration, Writing – review and editing

Author ORCIDs

Kwun Nok Mimi Man http://orcid.org/0000-0002-0132-9129
Peter Bartels http://orcid.org/0000-0001-5852-1835
Madeline Nieves-Cintron http://orcid.org/0000-0003-1935-8400
Manuel F Navedo http://orcid.org/0000-0001-6864-6594
Johannes W Hell http://orcid.org/0000-0001-7960-7531

Ethics

All procedures followed NIH guidelines and had been approved by the Institutional Animal Care and Use Committees (IACUC) at UC Davis (Protocol #20673 and #22403).

Decision letter and Author response
Decision letter https://doi.org/10.7554/eLife.79648.sa1
Author response https://doi.org/10.7554/eLife.79648.sa2

Additional files

Supplementary files

- Supplementary file 1. Amino acid residues of fragments of intracellular loops of $Ca_V1.2$ α_1-subunit used in GST pulldown studies.
- Supplementary file 2. Antibody dilutions used for immunoblotting.
- Supplementary file 3. shRNA sequences targeting rat Pyk2 and Src.
- Supplementary file 4. Sequencing primers for validation of knockdown constructs.
- MDAR checklist

Data availability

Raw datasets are available on Dryad (https://doi.org/10.25338/B86G9K).

The following dataset was generated:

Author(s)	Year	Dataset title	Dataset URL	Database and Identifier
Man K, Bartels P, Henderson PB, Kim K, Shi M, Zhang M, Ho S, Nieves-Cintron M, Navedo MF, Horne MC, Hell JW	2023	Raw data for Manuscript entitled "Alpha-1 adrenergic receptor - PKC - Pyk2 - Src signaling boosts L-type Ca2+ channel Cav1.2 activity and long-term potentiation in rodents"	https://dx.doi.org/10.25338/B86G9K	Dryad Digital Repository, 10.25338/B86G9K

References

Avraham H, Park SY, Schinkmann K, Avraham S. 2000. RAFTK/Pyk2-mediated cellular signalling. *Cellular Signalling* **12**:123–133. DOI: https://doi.org/10.1016/s0898-6568(99)00076-5, PMID: 10704819

Balijepalli RC, Foell JD, Hall DD, Hell JW, Kamp TJ. 2006. From the cover: localization of cardiac L-type Ca2+ channels to a caveolar macromolecular signaling complex is required for Beta2-adrenergic regulation. *PNAS* **103**:7500–7505. DOI: https://doi.org/10.1073/pnas.0503465103, PMID: 16648270

Bari A, Robbins TW. 2013. Noradrenergic versus dopaminergic modulation of Impulsivity, attention and monitoring behaviour in rats performing the stop-signal task: possible relevance to ADHD. *Psychopharmacology* **230**:89–111. DOI: https://doi.org/10.1007/s00213-013-3141-6, PMID: 23681165

Bartels P, Yu D, Huang H, Hu Z, Herzig S, Soong TW. 2018. Alternative splicing at N terminus and domain I modulates Ca(V)1.2 inactivation and surface expression. *Biophysical Journal* **115**:163. DOI: https://doi.org/10.1016/j.bpj.2018.06.001, PMID: 29972807

Bartos JA, Ulrich JD, Li H, Beazely MA, Chen Y, Macdonald JF, Hell JW. 2010. Postsynaptic clustering and activation of Pyk2 by PSD-95. *The Journal of Neuroscience* **30**:449–463. DOI: https://doi.org/10.1523/JNEUROSCI.4992-08.2010, PMID: 20071509

Bean BP, Nowycky MC, Tsien RW. 1984. Beta-adrenergic modulation of calcium channels in frog ventricular heart cells. *Nature* **307**:371–375. DOI: https://doi.org/10.1038/307371a0, PMID: 6320002

Bence-Hanulec KK, Marshall J, Blair LA. 2000. Potentiation of neuronal L calcium channels by IGF-1 requires phosphorylation of the Alpha1 subunit on a specific tyrosine residue. *Neuron* **27**:121–131. DOI: https://doi.org/10.1016/s0896-6273(00)00014-3, PMID: 10939336

Bennin DA, Don ASA, Brake T, McKenzie JL, Rosenbaum H, Ortiz L, DePaoli-Roach AA, Horne MC. 2002. Cyclin G2 Associates with protein phosphatase 2A catalytic and regulatory B' subunits in active complexes and induces nuclear aberrations and a G1/S phase cell cycle arrest. *The Journal of Biological Chemistry* **277**:27449–27467. DOI: https://doi.org/10.1074/jbc.M111693200, PMID: 11956189

Berkefeld H, Sailer CA, Bildl W, Rohde V, Thumfart JO, Eble S, Klugbauer N, Reisinger E, Bischofberger J, Oliver D, Knaus HG, Schulte U, Fakler B. 2006. BKca-Cav channel complexes mediate rapid and localized Ca2+-activated K+ signaling. *Science* **314**:615–620. DOI: https://doi.org/10.1126/science.1132915, PMID: 17068255

Berman DE, Dudai Y. 2001. Memory extinction, learning anew, and learning the new: Dissociations in the molecular machinery of learning in cortex. *Science* **291**:2417–2419. DOI: https://doi.org/10.1126/science.1058165, PMID: 11264539

Berridge CW, Shumsky JS, Andrzejewski ME, McGaughy JA, Spencer RC, Devilbiss DM, Waterhouse BD. 2012. Differential sensitivity to psychostimulants across prefrontal cognitive tasks: Differential involvement of noradrenergic α1- and α2-receptors. *Biological Psychiatry* **71**:467–473. DOI: https://doi.org/10.1016/j.biopsych.2011.07.022

Bhat S, Dao DT, Terrillion CE, Arad M, Smith RJ, Soldatov NM, Gould TD. 2012. Cacna1C (Cav1.2) in the pathophysiology of psychiatric disease. *Progress in Neurobiology* **99**:1–14. DOI: https://doi.org/10.1016/j.pneurobio.2012.06.001, PMID: 22705413

Bkaily G, Wang S, Bui M, Menard D. 1995. ET-1 stimulates Ca2+ currents in cardiac cells. *Journal of Cardiovascular Pharmacology* **26**:S293–S296. DOI: https://doi.org/10.1097/00005344-199506263-00088

Bloodgood BL, Sabatini BL. 2007. Nonlinear regulation of unitary synaptic signals by Cav(2.3) voltage-sensitive calcium channels located in dendritic spines. *Neuron* **53**:249–260. DOI: https://doi.org/10.1016/j.neuron.2006.12.017, PMID: 17224406

Bolshakov VY, Siegelbaum SA. 1994. Postsynaptic induction and presynaptic expression of hippocampal long-term depression. *Science* **264**:1148–1152. DOI: https://doi.org/10.1126/science.7909958, PMID: 7909958

Boric K, Muñoz P, Gallagher M, Kirkwood A. 2008. Potential adaptive function for altered long-term potentiation mechanisms in aging hippocampus. *The Journal of Neuroscience* **28**:8034–8039. DOI: https://doi.org/10.1523/JNEUROSCI.2036-08.2008, PMID: 18685028

Boudreau RL, Davidson BL. 2012. Generation of hairpin-based RNAi vectors for biological and therapeutic application. *Methods in Enzymology* **507**:275–296. DOI: https://doi.org/10.1016/B978-0-12-386509-0.00014-4, PMID: 22365779

Cahill L, Prins B, Weber M, McGaugh JL. 1994. Beta-adrenergic activation and memory for emotional events. *Nature* **371**:702–704. DOI: https://doi.org/10.1038/371702a0, PMID: 7935815

Carter ME, Yizhar O, Chikahisa S, Nguyen H, Adamantidis A, Nishino S, Deisseroth K, de Lecea L. 2010. Tuning arousal with optogenetic modulation of locus coeruleus neurons. *Nature Neuroscience* **13**:1526–1533. DOI: https://doi.org/10.1038/nn.2682, PMID: 21037585

Catterall WA. 2000. Structure and regulation of voltage-gated ca^{2+} channels. *Annual Review of Cell and Developmental Biology* **16**:521–555. DOI: https://doi.org/10.1146/annurev.cellbio.16.1.521, PMID: 11031246

Cavuş I, Teyler T. 1996. Two forms of long-term potentiation in area Ca1 activate different signal transduction cascades. *Journal of Neurophysiology* **76**:3038–3047. DOI: https://doi.org/10.1152/jn.1996.76.5.3038, PMID: 8930253

Chao JT, Gui P, Zamponi GW, Davis GE, Davis MJ. 2011. Spatial association of the Cav1.2 calcium channel with α5β1-integrin. *American Journal of Physiology. Cell Physiology* **300**:C477–C489. DOI: https://doi.org/10.1152/ajpcell.00171.2010, PMID: 21178109

Cheng TH, Chang CY, Wei J, Lin CI. 1995. Effects of endothelin 1 on calcium and sodium currents in isolated human cardiac myocytes. *Canadian Journal of Physiology and Pharmacology* **73**:1774–1783. DOI: https://doi.org/10.1139/y95-242, PMID: 8834492

Cheng JJ, Chao YJ, Wang DL. 2002. Cyclic strain activates redox-sensitive proline-rich tyrosine kinase 2 (Pyk2) in endothelial cells. *The Journal of Biological Chemistry* **277**:48152–48157. DOI: https://doi.org/10.1074/jbc.M110937200, PMID: 12368297

Choi J-H, Sim S-E, Kim J, Choi DI, Oh J, Ye S, Lee J, Kim T, Ko H-G, Lim C-S, Kaang B-K. 2018. Interregional synaptic maps among engram cells underlie memory formation. *Science* **360**:430–435 . DOI: https://doi.org/10.1126/science.aas9204

Clifton DR, Fields KA, Grieshaber SS, Dooley CA, Fischer ER, Mead DJ, Carabeo RA, Hackstadt T. 2004. A chlamydial type III translocated protein is tyrosine-phosphorylated at the site of entry and associated with recruitment of actin. *PNAS* **101**:10166–10171. DOI: https://doi.org/10.1073/pnas.0402829101, PMID: 15199184

Corvol J-C, Valjent E, Toutant M, Enslen H, Irinopoulou T, Lev S, Hervé D, Girault J-A. 2005. Depolarization activates ERK and proline-rich tyrosine kinase 2 (Pyk2) independently in different cellular compartments in hippocampal slices. *The Journal of Biological Chemistry* **280**:660–668. DOI: https://doi.org/10.1074/jbc.M411312200, PMID: 15537634

Dai S, Hall DD, Hell JW. 2009. Supramolecular assemblies and localized regulation of voltage-gated ion channels. *Physiological Reviews* **89**:411–452. DOI: https://doi.org/10.1152/physrev.00029.2007, PMID: 19342611

Davare MA, Dong F, Rubin CS, Hell JW. 1999. The A-kinase anchor protein Map2B and cAMP-dependent protein kinase are associated with class C L-type calcium channels in neurons. *The Journal of Biological Chemistry* **274**:30280–30287. DOI: https://doi.org/10.1074/jbc.274.42.30280, PMID: 10514522

Davare MA, Horne MC, Hell JW. 2000. Protein phosphatase 2A is associated with class C L-type calcium channels (Cav1.2) and Antagonizes channel phosphorylation by cAMP-dependent protein kinase. *The Journal of Biological Chemistry* **275**:39710–39717. DOI: https://doi.org/10.1074/jbc.M005462200, PMID: 10984483

Davare MA, Avdonin V, Hall DD, Peden EM, Burette A, Weinberg RJ, Horne MC, Hoshi T, Hell JW. 2001. A β2 adrenergic receptor signaling complex assembled with the Ca2+ channel Cav1.2. *Science* **293**:98–101. DOI: https://doi.org/10.1126/science.293.5527.98, PMID: 11441182

Davare MA, Hell JW. 2003. Increased phosphorylation of the neuronal L-type Ca(2+) channel Ca(V)1.2 during aging. *PNAS* **100**:16018–16023. DOI: https://doi.org/10.1073/pnas.2236970100, PMID: 14665691

Deyo RA, Straube KT, Disterhoft JF. 1989. Nimodipine facilitates associative learning in aging rabbits. *Science* **243**:809–811. DOI: https://doi.org/10.1126/science.2916127, PMID: 2916127

Dikic I, Tokiwa G, Lev S, Courtneidge SA, Schlessinger J. 1996. A role for Pyk2 and SRC in linking G-protein-coupled receptors with MAP kinase activation. *Nature* **383**:547–550. DOI: https://doi.org/10.1038/383547a0, PMID: 8849729

Dikic I, Dikic I, Schlessinger J. 1998. Identification of a new Pyk2 Isoform implicated in chemokine and antigen receptor signaling. *The Journal of Biological Chemistry* **273**:14301–14308. DOI: https://doi.org/10.1074/jbc.273.23.14301, PMID: 9603937

Disterhoft JF, Gispen WH, Traber J, Khachaturian ZS. 1994. Calcium hypothesis of aging and dementia. *Ann N Y Acad Sci* **747**:11. DOI: https://doi.org/10.1111/j.1749-6632.1994.tb44398.x

Dittmer PJ, Dell'Acqua ML, Sather WA. 2014. Ca(2+)/calcineurin-dependent inactivation of neuronal L-type Ca(2+) channels requires priming by AKAP-anchored protein kinase A. *Cell Reports* **7**:1410–1416. DOI: https://doi.org/10.1016/j.celrep.2014.04.039, PMID: 24835998

Dodge-Kafka KL, Langeberg L, Scott JD. 2006. Compartmentation of cyclic nucleotide signaling in the heart: the role of A-kinase anchoring proteins. *Circulation Research* **98**:993–1001. DOI: https://doi.org/10.1161/01.RES.0000218273.91741.30, PMID: 16645149

Dolmetsch RE, Pajvani U, Fife K, Spotts JM, Greenberg ME. 2001. Signaling to the nucleus by an L-type calcium channel-calmodulin complex through the MAP kinase pathway. *Science* **294**:333–339. DOI: https://doi.org/10.1126/science.1063395, PMID: 11598293

Döşemeci A, Dhallan RS, Cohen NM, Lederer WJ, Rogers TB. 1988. Phorbol ester increases calcium current and simulates the effects of angiotensin II on cultured neonatal rat heart myocytes. *Circulation Research* **62**:347–357. DOI: https://doi.org/10.1161/01.res.62.2.347, PMID: 2448059

Eiki J, Saeki K, Nagano N, Iino T, Yonemoto M, Takayenoki-Iino Y, Ito S, Nishimura T, Sato Y, Bamba M, Watanabe H, Sasaki K, Ohyama S, Kanatani A, Nagase T, Yada T. 2009. A selective small molecule glucagon-like peptide-1 secretagogue acting via depolarization-coupled Ca(2+) influx. *The Journal of Endocrinology* **201**:361–367. DOI: https://doi.org/10.1677/JOE-08-0528, PMID: 19332449

Endoh T. 2005. Involvement of SRC tyrosine kinase and mitogen-activated protein kinase in the Facilitation of calcium channels in rat nucleus of the tractus solitarius by angiotensin II. *The Journal of Physiology* **568**:851–865. DOI: https://doi.org/10.1113/jphysiol.2005.095307, PMID: 16123104

Ferreira MAR, O'Donovan MC, Meng YA, Jones IR, Ruderfer DM, Jones L, Fan J, Kirov G, Perlis RH, Green EK, Smoller JW, Grozeva D, Stone J, Nikolov I, Chambert K, Hamshere ML, Nimgaonkar VL, Moskvina V, Thase ME, Caesar S, et al. 2008. Collaborative genome-wide Association analysis supports a role for Ank3 and Cacna1C in bipolar disorder. *Nature Genetics* **40**:1056–1058. DOI: https://doi.org/10.1038/ng.209

Frangioni JV, Neel BG. 1993. Solubilization and purification of enzymatically active glutathione S-transferase (pGEX) fusion proteins. *Analytical Biochemistry* **210**:179–187. DOI: https://doi.org/10.1006/abio.1993.1170, PMID: 8489015

Fu Y, Westenbroek RE, Scheuer T, Catterall WA. 2013. Phosphorylation sites required for regulation of cardiac calcium channels in the fight-or-flight response. *PNAS* **110**:19621–19626. DOI: https://doi.org/10.1073/pnas.1319421110

Fu Y, Westenbroek RE, Scheuer T, Catterall WA. 2014. Basal and beta-adrenergic regulation of the cardiac calcium channel Cav1.2 requires phosphorylation of Serine 1700. *PNAS* **111**:16598–16603. DOI: https://doi.org/10.1073/pnas.1419129111, PMID: 25368181

Fuller MD, Emrick MA, Sadilek M, Scheuer T, Catterall WA. 2010. Molecular mechanism of calcium channel regulation in the fight-or-flight response. *Science Signaling* **3**:ra70. DOI: https://doi.org/10.1126/scisignal.2001152, PMID: 20876873

Gao T, Cuadra AE, Ma H, Bünemann M, Gerhardstein BL, Cheng T, Eick RT, Hosey MM. 2001. C-terminal fragments of the α1C(CaV1.2) subunit associate with and regulate L-type calcium channels containing C-terminal-truncated α1CSubunits. *Journal of Biological Chemistry* **276**:21089–21097. DOI: https://doi.org/10.1074/jbc.M008000200

Ghosh D, Syed AU, Prada MP, Nystoriak MA, Santana LF, Nieves-Cintrón M, Navedo MF. 2017. Calcium channels in vascular smooth muscle. *Advances in Pharmacology* **78**:49–87. DOI: https://doi.org/10.1016/bs.apha.2016.08.002, PMID: 28212803

Giustino TF, Maren S. 2018. Noradrenergic modulation of fear conditioning and extinction. *Frontiers in Behavioral Neuroscience* **12**:43. DOI: https://doi.org/10.3389/fnbeh.2018.00043, PMID: 29593511

Green EK, Grozeva D, Jones I, Jones L, Kirov G, Caesar S, Gordon-Smith K, Fraser C, Forty L, Russell E, Hamshere ML, Moskvina V, Nikolov I, Farmer A, McGuffin P, Wellcome Trust Case Control Consortium, Holmans PA, Owen MJ, O'Donovan MC, Craddock N. 2010. The bipolar disorder risk allele at *CACNA1C* also confers risk of recurrent major depression and of schizophrenia. *Molecular Psychiatry* **15**:1016–1022. DOI: https://doi.org/10.1038/mp.2009.49

Grover LM, Teyler TJ. 1990. Two components of long-term potentiation induced by different patterns of afferent activation. *Nature* **347**:477–479. DOI: https://doi.org/10.1038/347477a0, PMID: 1977084

Gui P, Wu X, Ling S, Stotz SC, Winkfein RJ, Wilson E, Davis GE, Braun AP, Zamponi GW, Davis MJ. 2006. Integrin receptor activation triggers converging regulation of Cav1.2 calcium channels by C-SRC and protein kinase A pathways. *The Journal of Biological Chemistry* **281**:14015–14025. DOI: https://doi.org/10.1074/jbc.M600433200, PMID: 16554304

Hahn B, Stolerman IP. 2005. Modulation of nicotine-induced attentional enhancement in rats by adrenoceptor antagonists. *Psychopharmacology* **177**:438–447. DOI: https://doi.org/10.1007/s00213-004-1969-5, PMID: 15252705

Hall DD, Feekes JA, Arachchige Don AS, Shi M, Hamid J, Chen L, Strack S, Zamponi GW, Horne MC, Hell JW. 2006. Binding of protein phosphatase 2A to the L-type calcium channel Cav1.2 next to Ser1928, its main PKA site, is critical for Ser1928 Dephosphorylation. *Biochemistry* **45**:3448–3459. DOI: https://doi.org/10.1021/bi051593z, PMID: 16519540

Hall DD, Davare MA, Shi M, Allen ML, Weisenhaus M, McKnight GS, Hell JW. 2007. Critical role of cAMP-dependent protein kinase anchoring to the L-type calcium channel Cav1.2 via A-kinase anchor protein 150 in neurons. *Biochemistry* **46**:1635–1646. DOI: https://doi.org/10.1021/bi062217x, PMID: 17279627

Hall DD, Dai S, Tseng PY, Malik Z, Nguyen M, Matt L, Schnizler K, Shephard A, Mohapatra DP, Tsuruta F, Dolmetsch RE, Christel CJ, Lee A, Burette A, Weinberg RJ, Hell JW. 2013. Competition between A-Actinin and Ca^{2+}-Calmodulin controls surface retention of the L-type Ca^{2+} channel Ca(V)1.2 . *Neuron* **78**:483–497. DOI: https://doi.org/10.1016/j.neuron.2013.02.032, PMID: 23664615

Harper SQ, Staber PD, Beck CR, Fineberg SK, Stein C, Ochoa D, Davidson BL. 2006. Optimization of feline immunodeficiency virus vectors for RNA interference. *Journal of Virology* **80**:9371–9380. DOI: https://doi.org/10.1128/JVI.00958-06, PMID: 16973543

He JQ, Pi Y, Walker JW, Kamp TJ. 2000. Endothelin-1 and Photoreleased Diacylglycerol increase L-type Ca2+ current by activation of protein kinase C in rat ventricular myocytes. *The Journal of Physiology* **524 Pt 3**:807–820. DOI: https://doi.org/10.1111/j.1469-7793.2000.00807.x, PMID: 10790160

Hell JW, Westenbroek RE, Warner C, Ahlijanian MK, Prystay W, Gilbert MM, Snutch TP, Catterall WA. 1993a. Identification and differential subcellular localization of the neuronal class C and class D L-type calcium channel A1 subunits. *The Journal of Cell Biology* **123**:949–962. DOI: https://doi.org/10.1083/jcb.123.4.949, PMID: 8227151

Hell JW, Yokoyama CT, Wong ST, Warner C, Snutch TP, Catterall WA. 1993b. Differential Phosphorylation of two size forms of the neuronal class C L-type calcium channel A1 subunit. *The Journal of Biological Chemistry* **268**:19451–19457 PMID: 8396138.

Hell JW, Yokoyama CT, Breeze LJ, Chavkin C, Catterall WA. 1995. Phosphorylation of Presynaptic and postsynaptic calcium channels by cAMP-dependent protein kinase in hippocampal neurons. *The EMBO Journal* **14**:3036–3044. DOI: https://doi.org/10.1002/j.1460-2075.1995.tb07306.x, PMID: 7621818

Hell JW, Westenbroek RE, Breeze LJ, Wang KKW, Chavkin C, Catterall WA. 1996. N-methyl-D-aspartate receptor-induced proteolytic conversion of postsynaptic class C L-type calcium channels in hippocampal neurons. *PNAS* **93**:3362–3367. DOI: https://doi.org/10.1073/pnas.93.8.3362, PMID: 8622942

Hoogland TM, Saggau P. 2004. Facilitation of L-type Ca2+ channels in Dendritic spines by activation of Beta2 adrenergic receptors. *The Journal of Neuroscience* **24**:8416–8427. DOI: https://doi.org/10.1523/JNEUROSCI.1677-04.2004, PMID: 15456814

Horn R. 1991. Estimating the number of channels in patch recordings. *Biophysical Journal* **60**:433–439. DOI: https://doi.org/10.1016/S0006-3495(91)82069-0

Hu XQ, Singh N, Mukhopadhyay D, Akbarali HI. 1998. Modulation of voltage-dependent Ca2+ channels in Rabbit Colonic smooth muscle cells by C-SRC and focal adhesion kinase. *Journal of Biological Chemistry* **273**:5337–5342. DOI: https://doi.org/10.1074/jbc.273.9.5337

Hu H, Real E, Takamiya K, Kang MG, Ledoux J, Huganir RL, Malinow R. 2007. Emotion enhances learning via norepinephrine regulation of AMPA-receptor trafficking. *Cell* **131**:160–173. DOI: https://doi.org/10.1016/j.cell.2007.09.017

Huang Y-Q, Lu W-Y, Ali DW, Pelkey KA, Pitcher GM, Lu YM, Aoto H, Roder JC, Sasaki T, Salter MW, MacDonald JF. 2001. Cakbeta/Pyk2 kinase is a signaling link for induction of long-term potentiation in Ca1 hippocampus. *Neuron* **29**:485–496. DOI: https://doi.org/10.1016/S0896-6273(01)00220-3

Hvoslef-Eide M, Oomen CA, Fisher BM, Heath CJ, Robbins TW, Saksida LM, Bussey TJ. 2015. Facilitation of spatial working memory performance following intra-Prefrontal cortical administration of the adrenergic Alpha1 agonist phenylephrine. *Psychopharmacology* **232**:4005–4016. DOI: https://doi.org/10.1007/s00213-015-4038-3

Jacquemet G, Baghirov H, Georgiadou M, Sihto H, Peuhu E, Cettour-Janet P, He T, Perälä M, Kronqvist P, Joensuu H, Ivaska J. 2016. L-type calcium channels regulate Filopodia stability and cancer cell invasion downstream of integrin signalling. *Nature Communications* **7**:13297. DOI: https://doi.org/10.1038/ncomms13297, PMID: 27910855

Jinnah HA, Yitta S, Drew T, Kim BS, Visser JE, Rothstein JD. 1999. Calcium channel activation and self-biting in mice. *PNAS* **96**:15228–15232. DOI: https://doi.org/10.1073/pnas.96.26.15228, PMID: 10611367

Jordan M, Schallhorn A, Wurm FM. 1996. Transfecting mammalian cells: optimization of critical parameters affecting calcium-phosphate precipitate formation. *Nucleic Acids Research* **24**:596–601. DOI: https://doi.org/10.1093/nar/24.4.596, PMID: 8604299

Kamp TJ, Hell JW. 2000. Regulation of cardiac L-type calcium channels by protein kinase A and protein kinase C. *Circulation Research* **87**:1095–1102. DOI: https://doi.org/10.1161/01.res.87.12.1095, PMID: 11110765

Klauck TM, Faux MC, Labudda K, Langeberg LK, Jaken S, Scott JD. 1996. Coordination of three signaling enzymes by AKAP79, a mammalian scaffold protein. *Science* **271**:1589–1592 . DOI: https://doi.org/10.1126/science.271.5255.1589, PMID: 8599116

Lacerda AE, Rampe D, Brown AM. 1988. Effects of protein kinase C Activators on cardiac ca^{2+} channels. *Nature* **335**:249–251. DOI: https://doi.org/10.1038/335249a0, PMID: 2457814

Lakkakorpi PT, Bett AJ, Lipfert L, Rodan GA, Duong LT. 2003. Pyk2 Autophosphorylation, but not kinase activity, is necessary for adhesion-induced association with C-SRC, Osteoclast spreading, and bone Resorption. *The Journal of Biological Chemistry* **278**:11502–11512. DOI: https://doi.org/10.1074/jbc.M206579200, PMID: 12514172

Leitch B, Szostek A, Lin R, Shevtsova O. 2009. Subcellular distribution of L-type calcium channel subtypes in rat hippocampal neurons. *Neuroscience* **164**:641–657. DOI: https://doi.org/10.1016/j.neuroscience.2009.08.006, PMID: 19665524

Lemke T, Welling A, Christel CJ, Blaich A, Bernhard D, Lenhardt P, Hofmann F, Moosmang S. 2008. Unchanged beta-adrenergic stimulation of cardiac L-type calcium channels in ca V 1.2 Phosphorylation site S1928A mutant mice. *The Journal of Biological Chemistry* **283**:34738–34744. DOI: https://doi.org/10.1074/jbc.M804981200, PMID: 18829456

Leonard AS, Hell JW. 1997. Cyclic AMP-dependent protein kinase and protein kinase C Phosphorylate N-methyl-D-aspartate receptors at different sites. *The Journal of Biological Chemistry* **272**:12107–12115. DOI: https://doi.org/10.1074/jbc.272.18.12107, PMID: 9115280

Lev S, Moreno H, Martinez R, Canoll P, Peles E, Musacchio JM, Plowman GD, Rudy B, Schlessinger J. 1995. Protein tyrosine kinase Pyk2 involved in Ca(2+)-Induced regulation of ion channel and MAP kinase functions. *Nature* **376**:737–745. DOI: https://doi.org/10.1038/376737a0, PMID: 7544443

Li X, Dy RC, Cance WG, Graves LM, Earp HS. 1999. Interactions between two cytoskeleton-associated tyrosine Kinases: calcium-dependent tyrosine kinase and focal adhesion tyrosine kinase. *The Journal of Biological Chemistry* **274**:8917–8924. DOI: https://doi.org/10.1074/jbc.274.13.8917, PMID: 10085136

Li H, Pink MD, Murphy JG, Stein A, Dell'Acqua ML, Hogan PG. 2012. Balanced interactions of calcineurin with Akap79 regulate Ca2+-Calcineurin-NFAT signaling. *Nature Structural & Molecular Biology* **19**:337–345. DOI: https://doi.org/10.1038/nsmb.2238

Li B, Tadross MR, Tsien RW. 2016. Sequential ionic and conformational signaling by calcium channels drives neuronal gene expression. *Science* **351**:863–867 . DOI: https://doi.org/10.1126/science.aad3647

Liu YP, Lin YL, Chuang CH, Kao YC, Chang ST, Tung CS. 2009. Alpha adrenergic modulation on effects of norepinephrine transporter inhibitor Reboxetine in five-choice serial reaction time task. *Journal of Biomedical Science* **16**:72. DOI: https://doi.org/10.1186/1423-0127-16-72, PMID: 19678962

Liu G, Papa A, Katchman AN, Zakharov SI, Roybal D, Hennessey JA, Kushner J, Yang L, Chen B-X, Kushnir A, Dangas K, Gygi SP, Pitt GS, Colecraft HM, Ben-Johny M, Kalocsay M, Marx SO. 2020. Mechanism of adrenergic Cav1.2 stimulation revealed by proximity Proteomics. *Nature* **577**:695–700. DOI: https://doi.org/10.1038/s41586-020-1947-z, PMID: 31969708

Ma H, Groth RD, Cohen SM, Emery JF, Li B, Hoedt E, Zhang G, Neubert TA, Tsien RW. 2014. gammaCaMKII Shuttles Ca(2+)/Cam to the nucleus to trigger CREB Phosphorylation and gene expression . *Cell* **159**:281–294. DOI: https://doi.org/10.1016/j.cell.2014.09.019, PMID: 25303525

Magee JC, Johnston D. 1997. A synaptically controlled, associative signal for hebbian plasticity in hippocampal neurons. *Science* **275**:209–213 . DOI: https://doi.org/10.1126/science.275.5297.209, PMID: 8985013

Man KNM, Navedo MF, Horne MC, Hell JW. 2020. B_2 adrenergic receptor complexes with the L-type ca^{2+} channel $ca_V1.2$ and AMPA-type glutamate receptors: paradigms for pharmacological targeting of protein interactions. *Annual Review of Pharmacology and Toxicology* **60**:155–174. DOI: https://doi.org/10.1146/annurev-pharmtox-010919-023404, PMID: 31561738

Marrion NV, Tavalin SJ. 1998. Selective activation of ca^{2+}-Activated K^+ channels by Co-localized ca^{2+}channels in hippocampal neurons. *Nature* **395**:900–905. DOI: https://doi.org/10.1038/27674, PMID: 9804423

Marshall MR, Clark JP III, Westenbroek R, Yu FH, Scheuer T, Catterall WA. 2011. Functional roles of a C-terminal signaling complex of Cav1 channels and A-kinase anchoring protein 15 in brain neurons. *Journal of Biological Chemistry* **286**:12627–12639. DOI: https://doi.org/10.1074/jbc.M110.175257

McHugh D, Sharp EM, Scheuer T, Catterall WA. 2000. Inhibition of cardiac L-type calcium channels by protein kinase C Phosphorylation of two sites in the N-terminal domain. *PNAS* **97**:12334–12338. DOI: https://doi.org/10.1073/pnas.210384297, PMID: 11035786

Mikami A, Imoto K, Tanabe T, Niidome T, Mori Y, Takeshima H, Narumiya S, Numa S. 1989. Primary structure and functional expression of the cardiac dihydropyridine-sensitive calcium channel. *Nature* **340**:230–233. DOI: https://doi.org/10.1038/340230a0, PMID: 2474130

Minzenberg MJ, Watrous AJ, Yoon JH, Ursu S, Carter CS. 2008. Modafinil shifts human locus coeruleus to low-tonic, high-Phasic activity during functional MRI. *Science* **322**:1700–1702. DOI: https://doi.org/10.1126/science.1164908

Mogilnicka E, Czyrak A, Maj J. 1987. Dihydropyridine calcium channel antagonists reduce immobility in the Mouse behavioral despair test; antidepressants facilitate nifedipine action. *European Journal of Pharmacology* **138**:413–416. DOI: https://doi.org/10.1016/0014-2999(87)90480-8, PMID: 3622617

Mogilnicka E, Czyrak A, Maj J. 1988. BAY K 8644 enhances immobility in the Mouse behavioral despair test, an effect blocked by nifedipine. *European Journal of Pharmacology* **151**:307–311. DOI: https://doi.org/10.1016/0014-2999(88)90813-8

Moosmang S, Haider N, Klugbauer N, Adelsberger H, Langwieser N, Müller J, Stiess M, Marais E, Schulla V, Lacinova L, Goebbels S, Nave K-A, Storm DR, Hofmann F, Kleppisch T. 2005. Role of hippocampal Cav1.2 Ca2+ channels in NMDA receptor-independent synaptic plasticity and spatial memory. *The Journal of Neuroscience* **25**:9883–9892. DOI: https://doi.org/10.1523/JNEUROSCI.1531-05.2005, PMID: 16251435

Murphy JG, Sanderson JL, Gorski JA, Scott JD, Catterall WA, Sather WA, Dell'Acqua ML. 2014. AKAP-anchored PKA maintains neuronal L-type calcium channel activity and NFAT transcriptional signaling. *Cell Reports* **7**:1577–1588. DOI: https://doi.org/10.1016/j.celrep.2014.04.027

Mustafa T, Walsh J, Grimaldi M, Eiden LE. 2010. Pac1Hop receptor activation facilitates catecholamine secretion selectively through 2-APB-sensitive Ca(2+) channels in Pc12 cells. *Cellular Signalling* **22**:1420–1426. DOI: https://doi.org/10.1016/j.cellsig.2010.05.005, PMID: 20471475

Navedo MF, Amberg GC, Votaw VS, Santana LF. 2005. Constitutively active L-type Ca2+ channels. *PNAS* **102**:11112–11117. DOI: https://doi.org/10.1073/pnas.0500360102, PMID: 16040810

Navedo MF, Nieves-Cintrón M, Amberg GC, Yuan C, Votaw VS, Lederer WJ, McKnight GS, Santana LF. 2008. Akap150 is required for Stuttering persistent Ca2+ Sparklets and angiotensin II-induced hypertension. *Circulation Research* **102**:e1–e11. DOI: https://doi.org/10.1161/CIRCRESAHA.107.167809, PMID: 18174462

Nyegaard M, Demontis D, Foldager L, Hedemand A, Flint TJ, Sørensen KM, Andersen PS, Nordentoft M, Werge T, Pedersen CB, Hougaard DM, Mortensen PB, Mors O, Børglum AD. 2010. Cacna1C (Rs1006737) is associated with schizophrenia. *Molecular Psychiatry* **15**:119–121. DOI: https://doi.org/10.1038/mp.2009.69

Oliveria SF, Dell'Acqua ML, Sather WA. 2007. Akap79/150 anchoring of calcineurin controls neuronal L-type Ca(2+) channel activity and nuclear signaling. *Neuron* **55**:261–275. DOI: https://doi.org/10.1016/j.neuron.2007.06.032, PMID: 17640527

Panichello MF, Buschman TJ. 2021. Shared mechanisms underlie the control of working memory and attention. *Nature* **592**:601–605. DOI: https://doi.org/10.1038/s41586-021-03390-w, PMID: 33790467

Park SY, Avraham HK, Avraham S. 2004. RAFTK/Pyk2 activation is mediated by Trans-acting Autophosphorylation in a SRC-independent manner. *Journal of Biological Chemistry* **279**:33315–33322. DOI: https://doi.org/10.1074/jbc.M313527200

Patriarchi T, Qian H, Di Biase V, Malik ZA, Chowdhury D, Price JL, Hammes EA, Buonarati OR, Westenbroek RE, Catterall WA, Hofmann F, Xiang YK, Murphy GG, Chen C-Y, Navedo MF, Hell JW. 2016. Phosphorylation of Cav1.2 on S1928 Uncouples the L-type Ca2+ channel from the B2 adrenergic receptor. *The EMBO Journal* **35**:1330–1345. DOI: https://doi.org/10.15252/embj.201593409, PMID: 27103070

Puumala T, Riekkinen P Sr, Sirviö J. 1997. Modulation of vigilance and behavioral activation by Alpha-1 adrenoceptors in the rat. *Pharmacology, Biochemistry, and Behavior* **56**:705–712. DOI: https://doi.org/10.1016/s0091-3057(96)00408-x, PMID: 9130297

Qian H, Matt L, Zhang M, Nguyen M, Patriarchi T, Koval OM, Anderson ME, He K, Lee H-K, Hell JW. 2012. B2 adrenergic receptor supports prolonged Theta tetanus - induced LTP . *Journal of Neurophysiology* **107**:2703–2712. DOI: https://doi.org/10.1152/jn.00374.2011

Qian H, Patriarchi T, Price JL, Matt L, Lee B, Nieves-Cintrón M, Buonarati OR, Chowdhury D, Nanou E, Nystoriak MA, Catterall WA, Poomvanicha M, Hofmann F, Navedo MF, Hell JW. 2017. Phosphorylation of Ser1928 mediates the enhanced activity of the L-type Ca2+ channel Cav1.2 by the Beta2-adrenergic receptor in neurons. *Science Signaling* **10**:eaaf9659. DOI: https://doi.org/10.1126/scisignal.aaf9659, PMID: 28119465

Ramos BP, Arnsten AFT. 2007. Adrenergic pharmacology and cognition: focus on the Prefrontal cortex. *Pharmacology & Therapeutics* **113**:523–536. DOI: https://doi.org/10.1016/j.pharmthera.2006.11.006, PMID: 17303246

Reuter H. 1983. Calcium channel modulation by neurotransmitters, enzymes and drugs. *Nature* **301**:569–574. DOI: https://doi.org/10.1038/301569a0, PMID: 6131381

Robbins TW. 2002. The 5-choice serial reaction time task: behavioural pharmacology and functional neurochemistry. *Psychopharmacology* **163**:362–380. DOI: https://doi.org/10.1007/s00213-002-1154-7, PMID: 12373437

Roskoski R. 2015. Src protein-tyrosine kinase structure, mechanism, and small molecule inhibitors. *Pharmacological Research* **94**:9–25. DOI: https://doi.org/10.1016/j.phrs.2015.01.003, PMID: 25662515

Rueden CT, Schindelin J, Hiner MC, DeZonia BE, Walter AE, Arena ET, Eliceiri KW. 2017. Imagej2: Imagej for the next generation of scientific image data. *BMC Bioinformatics* **18**:529. DOI: https://doi.org/10.1186/s12859-017-1934-z, PMID: 29187165

Sabri A, Govindarajan G, Griffin TM, Byron KL, Samarel AM, Lucchesi PA. 1998. Calcium- and protein kinase C-dependent activation of the tyrosine kinase Pyk2 by angiotensin II in vascular smooth muscle. *Circulation Research* **83**:841–851. DOI: https://doi.org/10.1161/01.RES.83.8.841

Sanderson JL, Dell'Acqua ML. 2011. AKAP signaling complexes in regulation of excitatory synaptic plasticity. *The Neuroscientist* **17**:321–336. DOI: https://doi.org/10.1177/1073858410384740, PMID: 21498812

Sayas CL, Ariaens A, Ponsioen B, Moolenaar WH. 2006. GSK-3 is activated by the tyrosine kinase Pyk2 during Lpa1-mediated Neurite retraction . *Molecular Biology of the Cell* **17**:1834–1844. DOI: https://doi.org/10.1091/mbc.e05-07-0688

Shankar S, Teyler TJ, Robbins N. 1998. Aging Differentially alters forms of long-term potentiation in rat hippocampal area Ca1. *Journal of Neurophysiology* **79**:334–341. DOI: https://doi.org/10.1152/jn.1998.79.1.334, PMID: 9425202

Shi CS, Kehrl JH. 2004. Pyk2 Amplifies epidermal growth factor and C-SRC-induced Stat3 activation. *The Journal of Biological Chemistry* **279**:17224–17231. DOI: https://doi.org/10.1074/jbc.M311875200, PMID: 14963038

Sinnegger-Brauns MJ, Hetzenauer A, Huber IG, Renström E, Wietzorrek G, Berjukov S, Cavalli M, Walter D, Koschak A, Waldschütz R, Hering S, Bova S, Rorsman P, Pongs O, Singewald N, Striessnig J. 2004. Isoform-specific regulation of mood behavior and Pancreatic beta cell and cardiovascular function by L-type ca 2+ channels. *The Journal of Clinical Investigation* **113**:1430–1439. DOI: https://doi.org/10.1172/JCI20208, PMID: 15146240

Smoller JW. 2013. Disorders and borders: psychiatric Genetics and Nosology. *American Journal of Medical Genetics. Part B, Neuropsychiatric Genetics* **162B**:559–578. DOI: https://doi.org/10.1002/ajmg.b.32174, PMID: 24132891

Snutch TP, Leonard JP, Gilbert MM, Lester HA, Davidson N. 1990. Rat brain expresses a heterogeneous family of calcium channels. *PNAS* **87**:3391–3395. DOI: https://doi.org/10.1073/pnas.87.9.3391, PMID: 1692134

Snutch TP, Tomlinson WJ, Leonard JP, Gilbert MM. 1991. Distinct calcium channels are generated by alternative splicing and are Differentially expressed in the mammalian CNS. *Neuron* **7**:45–57. DOI: https://doi.org/10.1016/0896-6273(91)90073-9, PMID: 1648941

Sorokin A, Kozlowski P, Graves L, Philip A. 2001. Protein-tyrosine kinase Pyk2 mediates Endothelin-induced P38 MAPK activation in glomerular mesangial cells. *The Journal of Biological Chemistry* **276**:21521–21528. DOI: https://doi.org/10.1074/jbc.M008869200, PMID: 11278444

Splawski I, Timothy KW, Sharpe LM, Decher N, Kumar P, Bloise R, Napolitano C, Schwartz PJ, Joseph RM, Condouris K, Tager-Flusberg H, Priori SG, Sanguinetti MC, Keating MT. 2004. Ca(V)1.2 calcium channel dysfunction causes a Multisystem disorder including arrhythmia and autism. *Cell* **119**:19–31. DOI: https://doi.org/10.1016/j.cell.2004.09.011, PMID: 15454078

Strauss O, Mergler S, Wiederholt M. 1997. Regulation of L-type calcium channels by protein tyrosine kinase and protein kinase C in cultured rat and human retinal pigment epithelial cells. *FASEB Journal* **11**:859–867. DOI: https://doi.org/10.1096/fasebj.11.11.9285484, PMID: 9285484

Taylor SC, Green KN, Carpenter E, Peers C. 2000. Protein kinase C evokes Quantal catecholamine release from Pc12 cells via activation of L-type Ca2+ channels. *Journal of Biological Chemistry* **275**:26786–26791. DOI: https://doi.org/10.1016/S0021-9258(19)61444-4

Thibault O, Landfield PW. 1996. Increase in single L-type calcium channels in hippocampal neurons during aging. *Science* **272**:1017–1020 . DOI: https://doi.org/10.1126/science.272.5264.1017, PMID: 8638124

Tigaret CM, Olivo V, Sadowski JHLP, Ashby MC, Mellor JR. 2016. Coordinated activation of distinct Ca(2+) sources and Metabotropic glutamate receptors Encodes Hebbian synaptic plasticity. *Nature Communications* **7**:10289. DOI: https://doi.org/10.1038/ncomms10289, PMID: 26758963

Tigaret CM, Lin T-CE, Morrell ER, Sykes L, Moon AL, O'Donovan MC, Owen MJ, Wilkinson LS, Jones MW, Thomas KL, Hall J. 2021. Neurotrophin receptor activation rescues cognitive and synaptic abnormalities caused by hemizygosity of the psychiatric risk gene cacna1c. *Molecular Psychiatry* **26**:1748–1760 . DOI: https://doi.org/10.1038/s41380-020-01001-0

Tse KWK, Lin KBL, Dang-Lawson M, Guzman-Perez A, Aspnes GE, Buckbinder L, Gold MR. 2012. Small molecule inhibitors of the Pyk2 and FAK Kinases modulate Chemoattractant-induced migration, adhesion and AKT activation in follicular and marginal zone B cells. *Cellular Immunology* **275**:47–54. DOI: https://doi.org/10.1016/j.cellimm.2012.03.002, PMID: 22507871

Turner M, Anderson DE, Bartels P, Nieves-Cintron M, Coleman AM, Henderson PB, Man KNM, Tseng PY, Yarov-Yarovoy V, Bers DM, Navedo MF, Horne MC, Ames JB, Hell JW. 2020. α-Actinin-1 promotes activity of the L-type ca^{2+} channel ca_V 1.2. *The EMBO Journal* **39**:e102622. DOI: https://doi.org/10.15252/embj.2019102622, PMID: 31985069

Voelker TL, Del Villar SG, Westhoff M, Costa AD, Coleman AM, Hell JW, Horne MC, Dickson EJ, Dixon RE. 2023. Acute Phosphatidylinositol 4,5 Bisphosphate depletion Destabilizes sarcolemmal expression of cardiac L-type ca^{2+} channel ca_V1.2. *PNAS* **120**:e2221242120. DOI: https://doi.org/10.1073/pnas.2221242120, PMID: 36976770

Walter HJ, McMahon T, Dadgar J, Wang D, Messing RO. 2000. Ethanol regulates calcium channel subunits by protein kinase C Delta -Dependent and -Independent mechanisms. *Journal of Biological Chemistry* **275**:25717–25722. DOI: https://doi.org/10.1074/jbc.M910282199

Wang H, Ardiles AO, Yang S, Tran T, Posada-Duque R, Valdivia G, Baek M, Chuang Y-A, Palacios AG, Gallagher M, Worley P, Kirkwood A. 2016. Metabotropic glutamate receptors induce a form of LTP controlled by translation and arc signaling in the hippocampus. *The Journal of Neuroscience* **36**:1723–1729. DOI: https://doi.org/10.1523/JNEUROSCI.0878-15.2016

Ward SG, Reif K, Ley S, Fry MJ, Waterfield MD, Cantrell DA. 1992. Regulation of Phosphoinositide Kinases in T cells evidence that Phosphatidylinositol 3-kinase is not a substrate for T cell antigen receptor-regulated tyrosine Kinases. *The Journal of Biological Chemistry* **267**: –23869 PMID: 1385426.

Wheeler DG, Groth RD, Ma H, Barrett CF, Owen SF, Safa P, Tsien RW. 2012. Cav1 and Cav2 channels engage distinct modes of Ca2+ signaling to control CREB-dependent gene expression. *Cell* **149**:1112–1124. DOI: https://doi.org/10.1016/j.cell.2012.03.041, PMID: 22632974

White JA, McKinney BC, John MC, Powers PA, Kamp TJ, Murphy GG. 2008. Conditional forebrain deletion of the L-type calcium channel ca V 1.2 disrupts remote spatial memories in mice . *Learning & Memory* **15**:1–5. DOI: https://doi.org/10.1101/lm.773208

Whitlock JR, Heynen AJ, Shuler MG, Bear MF. 2006. Learning induces long-term potentiation in the hippocampus. *Science* **313**:1093–1097 . DOI: https://doi.org/10.1126/science.1128134

Wu X, Davis GE, Meininger GA, Wilson E, Davis MJ. 2001. Regulation of the L-type calcium channel by α5β1 integrin requires signaling between focal adhesion proteins. *Journal of Biological Chemistry* **276**:30285–30292. DOI: https://doi.org/10.1074/jbc.M102436200

Xu H, Ginsburg KS, Hall DD, Zimmermann M, Stein IS, Zhang M, Tandan S, Hill JA, Horne MC, Bers D, Hell JW. 2010. Targeting of protein phosphatases Pp2A and Pp2B to the C-terminus of the L-type calcium channel ca V1.2 . *Biochemistry* **49**:10298–10307. DOI: https://doi.org/10.1021/bi101018c

Yang L, Liu G, Zakharov SI, Morrow JP, Rybin VO, Steinberg SF, Marx SO. 2005. Ser1928 is a common site for Cav1.2 phosphorylation by protein kinase C isoforms. *Journal of Biological Chemistry* **280**:207–214. DOI: https://doi.org/10.1074/jbc.M410509200

Yang S, Roselli F, Patchev AV, Yu S, Almeida OFX. 2013. Non-receptor-tyrosine kinases integrate fast glucocorticoid signaling in hippocampal neurons. *Journal of Biological Chemistry* **288**:23725–23739. DOI: https://doi.org/10.1074/jbc.M113.470146

Zamponi GW, Striessnig J, Koschak A, Dolphin AC. 2015. The physiology, pathology, and pharmacology of voltage-gated calcium channels and their future therapeutic potential. *Pharmacological Reviews* **67**:821–870. DOI: https://doi.org/10.1124/pr.114.009654, PMID: 26362469

Zhao M, Finlay D, Zharkikh I, Vuori K. 2016. Novel role of SRC in priming Pyk2 phosphorylation. *PLOS ONE* **11**:e0149231. DOI: https://doi.org/10.1371/journal.pone.0149231, PMID: 26866924